Quaternary Science Reviews 271 (2021) 107191

Contents lists available at ScienceDirect

Quaternary Science Reviews

journal homepage: www.elsevier.com/locate/quascirev

Southern Ocean sea surface temperature synthesis: Part 1. Evaluation of temperature proxies at glacial-interglacial time scales

David Chandler*, Petra Langebroek

NORCE Norwegian Research Centre, Bjerknes Centre for Climate Research, Bergen, Norway

ARTICLE INFO

Article history:
Received 1 June 2021
Received in revised form
9 September 2021
Accepted 12 September 2021
Available online 1 October 2021

Handling Editor: I Hendy

Keywords:
Southern Ocean
Sea surface temperature (SST)
Proxy
Quaternary
Paleoclimate
Glacial
Interglacial

ABSTRACT

Quaternary interglacial climates are often used as analogues for how the Antarctic Ice Sheet will respond to future climate warming. Southern Ocean marine sediments provide an important paleoclimate archive in this respect. Sea surface temperature (SST) reconstructions in the Southern Ocean depend exclusively on the fossils or geochemical signatures of planktic organisms, but the strengths of these SST proxies remain poorly quantified in this region. To improve confidence in paleoclimate reconstructions, Part 1 of this two-part study evaluates the reliability of Southern Ocean SST proxies employed at Quaternary glacial-interglacial time scales, focusing on three key potential problems: advection/dispersion, seasonality, and non-thermal influences. We find that foraminifera assemblages and long-chain alkenones likely provide the most reliable SST reconstructions in this region. Diatom assemblages and the *Globigerina bulloides* Mg/Ca ratio are considered to be 'moderately' reliable. Both are subject to potentially significant non-thermal influences, and diatom assemblages are likely modified by species-dependent advection as they sink to the sea floor. Nevertheless, diatoms are valuable at higher latitudes, since alkenones and foraminifera assemblages lose sensitivity below ~1 to 2 °C. Dinocyst assemblages, radiolarian assemblages, GDGTs and *Neogloboquadrina pachyderma* Mg/Ca are considered the least reliable in the Southern Ocean, due to weak calibrations, poorly-constrained non-thermal influences, and/or strong advection bias. We note that the seasonality of all proxies remains poorly constrained. Overall, Southern Ocean SST reconstructions using the recommended proxies and calibrations should be robust when averaging across multiple sites and proxy types, but should be treated with caution when analysing spatial variability, a small number of sites, or a single proxy type. Quantifying the effect of advection should be a priority for all planktic groups employed in Southern Ocean paleoclimate reconstructions.

1. Introduction

Past interglacial climates are receiving increasing interest as analogues for near-future climate warming, and the resulting sea level contributions of ice sheets (e.g., Dutton et al., 2015; Yin and Berger, 2015; Sutter et al., 2016; Gilford et al., 2020; Turney et al., 2020; DeConto et al., 2021). While ice core evidence suggests that the East Antarctic Ice Sheet has persisted through several previous interglacials (Petit et al., 1999; Watanabe et al., 2003; Jouzel et al., 2007), the rate and extent of West Antarctic Ice Sheet retreat during interglacials remains debated (Mercer, 1978; Scherer et al., 1998; Vaughan, 2008; Turney et al., 2020). During the last interglacial (LIG), Southern mid-latitude sea surface temperatures (SSTs) and Antarctic surface air temperatures were likely less than ~2 °C and ~4 °C above present, respectively, while sea level likely reached 6–9 m above present (Kopp et al., 2009; Masson-Delmotte et al., 2011; Capron et al., 2014; Dutton et al., 2015; Hoffman et al., 2017). Individual contributions to this sea level high stand remain uncertain, but the potential for extensive West Antarctic Ice Sheet ice loss even under moderate future warming is of concern. Besides sea level rise, the regional and global climatic consequences of increasing fresh water fluxes from Antarctica into the Southern Ocean provide additional motivation for considering future ice loss (Bintanja et al., 2015; Fogwill et al., 2015; Mackie et al., 2020).

Interglacial paleoclimate reconstructions in the Southern Hemisphere mid to high latitudes are essential for understanding past ocean and ice sheet responses to warming, but are limited by the logistical challenges of retrieving marine sediment cores or ice cores from this remote region. Reconstructions are further hindered by a lack of ice-free land surfaces, resulting in a low diversity

* Corresponding author.
E-mail address: dcha@norceresearch.no (D. Chandler).

https://doi.org/10.1016/j.quascirev.2021.107191

of quantitative climatic information that can be reliably reconstructed on a large scale at glacial-interglacial time scales: principally SST north of ~60°S (Capron et al., 2014; Hoffman et al., 2017; Turney et al., 2020), sea-ice cover/duration (Crosta et al., 2005), and Antarctic surface air temperature at high elevations near ice divides (e.g., Petit et al., 1999; Jouzel et al., 2007; Masson-Delmotte et al., 2011). Existing SST syntheses for the LIG provide good benchmarks for evaluating climate simulations, and it is encouraging that their somewhat different approaches yield similar regional SST anomalies (Capron et al., 2014; Hoffman et al., 2017; Turney et al., 2020). However, given the strong dependence on SST reconstructions for understanding past climates in the Southern Ocean and Antarctica, confidence in these reconstructions is essential. Although Capron et al. (2014) and Hoffman et al. (2017) adopted rigorous approaches in their data selection and dating, they mostly used temperature reconstructions as originally published: these have employed many different calibrations and training datasets that are not necessarily optimal for the Southern Ocean.

The need for calibrations optimised for the Southern Ocean is motivated by the region's very different ocean dynamics when compared to those in the relatively discrete ocean basins of the northern high latitudes, which likely lead to different associations between SST and sub-polar ecosystems (e.g., Hunt et al., 2016). Clearly this is of importance since SST proxies rely solely on planktic organisms. Two key characteristics of the Southern Ocean are its rapid lateral advection and strong seasonality. The potential impacts of these on our SST reconstructions are considered in Sections 3 and 4. In Section 5 we briefly review the key characteristics of each proxy, and evaluate existing calibrations that are relevant to this region. This evaluation is helped by several recent global or regional core-top sediment databases (Tierney and Tingley, 2014, 2015, 2018, 2015; Haddam et al., 2016; Saenger and Evans, 2019; Tierney et al., 2019). On this basis we make some recommendations for which proxies and calibrations are considered most reliable for Southern Ocean SST reconstructions (Section 6). In the companion paper (Part 2: Chandler and Langebroek, 2021) we use these to reconstruct a Southern Ocean regional average SST anomaly focusing on the penultimate glacial cycle (marine isotope stages 6 and 5, ~190 to 80 ka before present).

2. Study region and methods

The study region, informally referred to here as the Southern Ocean, is the ocean south of 40°S. This northern limit minimises inter-basin variability by restricting our study area predominantly to a region that is rapidly mixed by the Antarctic Circumpolar Current (ACC). The chosen region also contains few continental margins, where transport in boundary currents can cause problems for proxy reconstructions (see Section 3). Southern Ocean dynamics and their links to global climate are described elsewhere (e.g., Rintoul, 2018), and the modern SST (Fig. S1.1) is taken from the 2018 World Ocean Atlas for the period 2005 to 2017 (WOA2018: Locarnini et al., 2018).

The seven SST proxies considered here are all retrieved from marine sediment cores. These comprise three geochemical proxies employing substances synthesized by planktic organisms (long-chain alkenones, glycerol dialkyl glycerol tetraethers, foraminiferal calcite Mg/Ca), and four proxies based on assemblages of the fossil planktic organisms themselves (diatoms, dinoflagellate cysts, foraminifera, radiolarians). The geochemical proxies require empirical calibrations to reconstruct SST, and the assemblages require a statistical approach using transfer functions, the modern analogue technique (MAT) or neural networks (e.g., Imbrie and Kipp, 1971; Hutson, 1980; Overpeck et al., 1985; Barrows and Juggins, 2005). We do not use planktic calcite $\delta^{18}O$ as an SST proxy because it is also dependent on local seawater $\delta^{18}O$, which changes over glacial-interglacial cycles (e.g., Urey et al., 1951; Shackleton, 1974).

Knowledge of how planktic organisms respond to temperature requires samples collected in-situ (plankton tows or sediment traps), experiments with live cultures in a laboratory, or samples of recent ocean sediments. Each of these has its own strengths and weaknesses, summarised in Table 1. Where possible, our approach here is to use core-top data to evaluate calibrations, since these best represent the samples in marine sediment cores. Data from laboratory experiments or in-situ sampling are also used to help assess the representative depth and seasonality, as well as non-thermal influences, that cannot be determined from core-top sediments.

3. Lateral advection by ocean currents and sediment drift

Planktic organisms are advected laterally in the ocean, during their lifetime near the surface and then as they sink through the water column. Post-depostional reworking by bottom currents and bioturbation can also transport fossils or biomarkers laterally away from their source region or vertically within the sediment. These potentially important sources of error are discussed below.

3.1. Lateral advection prior to deposition

Planktic organisms can travel a long distance – perhaps several hundred to >1000 km – prior to deposition, potentially introducing a considerable temperature error (Popova, 1986; Benthien and Müller, 2000; Rühlemann and Butzin, 2006; van Sebille et al., 2015; Nooteboom et al., 2019). The magnitude of the error depends on ocean circulation patterns and the sinking rate of planktic particles, and is not surprisingly higher for slower sinking particles or regions with strong temperature gradients (Nooteboom et al., 2019). Lateral advection has been used to explain some regional clusters of warm or cold residuals from global calibrations, particularly those associated with boundary currents (e.g., for alkenones: Rühlemann and Butzin, 2006; Tierney and Tingley, 2018).

The strongly zonal character of the ACC – *on average* – may suggest limited advection bias in the Southern Ocean, if particles are simply advected eastwards to regions of a similar latitude and SST. However, *instantaneous* velocity patterns show a complex pattern of eddies, even in parts of the Southern Ocean far from any boundary currents (Park et al., 2019, their Fig. 11). These eddies are an important component of the heat transport across the ACC (Volkov et al., 2010; Sun et al., 2019) and could be similarly effective at dispersing planktic organisms meridionally. In the Southern Ocean, eddy-resolving mesoscale ocean modelling suggests fast-sinking organisms such as foraminifera are most likely deposited in sediments where local SST is similar (within ~1 °C) to that where the organism started sinking (van Sebille et al., 2015; Nooteboom et al., 2019). However, slowly sinking particles travelling >1000 km are associated with SST offsets exceeding 10 °C between source and sedimentation site (Scenario 2: Nooteboom et al., 2019). This could introduce a considerable error in our reconstructed temperatures.

Turney et al. (2020) used back-trajectory calculations in an eddy-resolving ocean model to correct their LIG temperature reconstructions for 'footprint bias' caused by ocean drift, assuming a sinking rate of 200 m/day. Applying this correction to LIG marine sediment core sites revealed a globally variable footprint bias, including a consistently cold bias of up to 2 °C in the southern mid- to high-latitudes and a warm bias in the North Atlantic (see their Fig. 1). Despite its clear importance, this drift correction may not be appropriate in Southern Ocean SST reconstructions for four

Table 1
Some advantages and disadvantages of the main strategies for establishing calibrations or training data sets.

Calibration strategy	Advantages	Disadvantages
Laboratory cultures	Experiments under controlled conditions allows systematic evaluation of thermal and non-thermal influences. Can reveal functional form of calibration for geochemical proxies (e.g. linear/exponential). Can extend range of conditions beyond that of present climate.	Requires knowledge of organism's depth and seasonality to interpret temperature signal. Behaviour in culture may differ from in-situ, possibly missing important life-cycle stages (Barker et al., 2005; Rahul et al., 2015). Very different time scales to samples from marine sediments.
In-situ sampling: plankton tows, sediment traps, video plankton recorder	The only practical way to evaluate representative seasonality and depth of each organism. Different assemblages in sediment trap and underlying core-top samples highlight important problems with advection (e.g., for radiolarians: see Fig. 4 in Rigual-Hernández et al., 2016).	Logistics limit spatial and/or temporal resolution, and spatial and/or temporal coverage: observations over many years may be required to overcome high spatial or inter-annual variance (e.g., Ortiz and Mix, 1997; Kim and Orsi, 2014). Restricted range of conditions: may require extrapolation to past climates.
Core-top samples	Samples most closely matching those in marine sediment cores. Samples integrate conditions over many years of sedimentation, and thus include inter-annual variability (e.g., Ortiz and Mix, 1997; Kim and Orsi, 2014) and seasonal weighting.	Logistics limit spatial resolution. Restricted range of conditions: may require extrapolation to past climates. Poor age control: sample age could span hundreds or thousands of years. Non-thermal influences not easily evaluated. Seasonality and depth cannot be evaluated. Sediment provenance uncertain, due to horizontal advection or re-working (see Section 3). Spatially clustered sampling can lead to spatial autocorrelation and overestimate of calibration strength (see debate by Guiot and de Vernal, 2011a,b; Telford and Birks, 2011).

reasons.

1. It is not appropriate to apply the same drift correction to all proxies. Sinking rates vary by a factor of >100 (Fig. 1), and are poorly constrained for most planktic groups. Estimated sinking rates of 200 m/day are also too fast for some important groups.
2. Many SST calibrations, and all statistical reconstructions (MAT/ANN/transfer functions) are established empirically from modern ocean sediments, but without a drift correction, so the *mean regional bias due to drift under modern conditions* is already implicitly included in the calibration. Drift-correcting the reconstructed SSTs but not the calibration reference SSTs (especially if using an inappropriate sinking rate) risks adding bias, rather than reducing it.
3. The drift correction is most important where there are strong temperature gradients, for example close to ocean fronts and boundary currents (van Sebille et al., 2015; Nooteboom et al., 2019; Turney et al., 2020). Therefore, the modelled drift correction suffers from high sensitivity to the particular position of fronts in the ocean model, likely resulting in the greatest uncertainty in the correction coinciding with those regions where the correction is most needed. During past climates, the locations of fronts may have been very different to their modern locations. Consequently, temperature reconstructions will be influenced by subjective or uncertain ocean model configurations which add an unknown error that cannot be included in the reported temperature uncertainty.
4. Particle 'advection' also includes a diffusion component related to the eddy diffusivity of the ocean, which is a random process that cannot necessarily be reversed in back-trajectory modelling (e.g., Batchelder, 2006).

Here, we have summarised measurements of sinking rates (Fig. 1; Table S2.1), and evaluate which proxies may be most susceptible to advection bias in the Southern Ocean. Sinking rates can also be calculated from particle and water properties using simple formulae from fluid dynamics, but we only consider observations here because calculated sinking velocities often provide poor estimates when compared to observations (e.g., Laurenceau-Cornec et al., 2015).

Foraminifera are relatively fast sinkers (mostly >200 m/day: Fig. 1), and are the least likely to be affected by advection bias as they will likely be deposited within 1–3 weeks.

Sinking rates of radiolarians vary widely between species (13 to > 400 m/day: Fig. 1), but several important Southern Ocean taxa are mostly slow to moderate sinkers, at typically <100 m/day (Takahashi and Honjo, 1983). The combination of slow and variable sinking rates across this group means sedimentary radiolarian assemblages can be substantially altered relative to their ocean surface assemblage, since slow sinkers will travel much further than the moderate sinkers before deposition.

Individual diatoms sink very slowly (Fig. 1) but become aggregated into faster-sinking clumps ('marine snow') or into zooplankton faecal pellets (50–300 m/day); therefore, the effective diatom sinking rates are likely to be very process-dependent (Eppley et al., 1967; Shanks and Trent, 1980; Smetacek, 1985; Passow, 1991; Miklasz and Denny, 2010; Schmidt et al., 2014; Gemmell et al., 2016). Diatom-rich 'marine snow' sinking rates may also depend on species composition (Laurenceau-Cornec et al., 2015); this could significantly skew sedimentary assemblages. Given the slow sinking rate of individual diatoms, yet the relatively low RMSEP for this proxy (e.g., Esper and Gersonde, 2014), we suggest that sedimentary diatoms mostly reach the ocean floor in aggregates or faecal pellets. However, we are not confident in the validity of this assumption, and even these aggregates could still undergo significant advection in some regions.

Similarly to diatoms, dinocysts are slow sinkers as individuals (Anderson et al., 1985), but may be incorporated into faster sinking aggregates or in zooplankton fecal pellets. However, Nooteboom et al. (2019) have argued that most dinocysts reach sediments following the slow route.

Coccolithophores, which synthesise alkenones, are the slowest sinkers at < 0.6 m/day (Lecourt et al., 1996; Rosas-Navarro et al., 2018). Their success as a SST proxy is likely mediated by their incorporation into aggregates or zooplankton faecal pellets (Fig. 1). The extra mass provided by coccolith calcite can increase the sinking rate of organic aggregates (Schmidt et al., 2014), but again the aggregates could still undergo significant advection.

No direct sinking rate observations are available (to our knowledge) for Thaumarchaeota, the microbial organisms which synthesise GDGTs. However, analysis of sinking particles suggests GDGTs are exported in faecal pellets and marine snow (Yamamoto

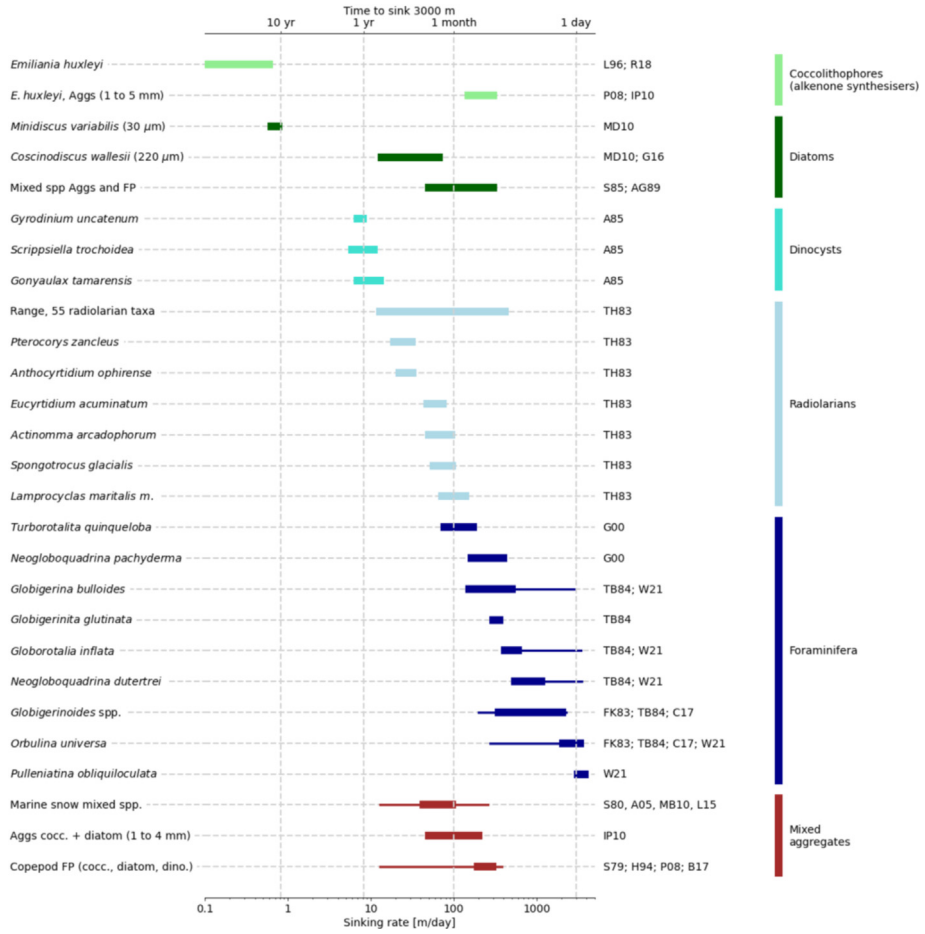

Fig. 1. Observed sinking rates of planktic organisms, as individuals or as aggregates (Aggs) and faecal pellets (FP). Thick lines show the 'likely' range and thin lines the upper and lower limits based on qualitative assessments of the cited observations. Sinking times (top axis) are estimated assuming a steady sinking rate in water 3000 m deep. References: S79 Small et al. (1979), S80 Shanks and Trent (1980), FK83 Fok-Pun and Komar (1983), TH83 Takahashi and Honjo (1983), TB84 Takahashi and Be (1984), A85 Anderson et al. (1985), S85 Smetacek (1985), AG89 Alldredge and Gotschalk (1989), H94 Harris (1994), L96 Lecourt et al. (1996), G00 von Gyldenfeldt et al. (2000), A05 Ashjian et al. (2005), P08 Ploug et al. (2008), IP10 Iversen and Ploug (2010), MB10 McDonnell and Buesseler (2010), MD10 Miklasz and Denny (2010), L15 Laurenceau-Cornec et al. (2015), G16 Gemmell et al. (2016), R18 Rosas-Navarro et al. (2018), B17 Belcher et al. (2017), C17 Caromel et al. (2014), W21 Walker et al. (2021).

et al., 2012). Thus, there could be some delay between GDGT synthesis and export if peak GDGT production is not synchronous with peak export, introducing potential for additional advection bias.

The apparent success of core-top SST calibrations for most of these proxy groups (see Section 5) does not mean that advection is not important. For example, advection could strongly modify the local radiolarian core-top assemblages in some regions under modern conditions, and this modification would then be empirically accounted for in MAT reconstructions, albeit contributing some increased variance. The real problem is then whether down-core changes in the assemblage reflect changes in advection (and provenance), rather than changes in local SST. The two groups with the highest confidence in this respect are foraminifera and coccolithophores. The former are fast sinkers and unlikely to be transported far from their origin, leading to a temperature offset typically <1 °C in the Southern Ocean (van Sebille et al., 2015). The latter are very slow sinkers as individuals and must reach sediments in faecal pellets; in addition, the excellent agreement between alkenone calibrations based on cultures, in-situ sampling and core-top sediments suggests advection is unlikely be a strong influence in general. However, even for this proxy, particular regions with strong meridional surface currents show high residuals from the global calibration (see Benthien and Müller, 2000; Tierney and Tingley, 2018, and Section 5.1 below).

3.2. Post-depositional drift

Post-depositional drift poses two additional problems for proxy-based reconstructions in marine sediments (e.g., Dezileau et al., 2000; Ohkouchi et al., 2002; Lüer et al., 2009). First, older or non-local sediments can become mixed with recent local sediments, for example following re-suspension and transport of older sediments by ocean bottom currents. This could affect age models as well as SST reconstructions, particularly when local sedimentation rates are low. Secondly, suspension and deposition of bottom sediments is grain size dependent, potentially skewing faunal assemblages, or resulting in different provenances of different proxies in the same core.

Due to the very site-specific conditions influencing sediment transport, the ocean modelling employed to quantify ocean advection bias cannot be used here. Instead, radiocarbon dating of different sediment components (e.g., different fossils or biomarkers) within the same sediment horizon helps evaluate which proxies might be most susceptible to drift. Some examples are as follows.

- Ohkouchi et al. (2002) found alkenone ^{14}C ages up to 7 kyr older than associated foraminifera in a drift deposit on the Bermuda

Rise. In continental shelf settings, alkenones were −1 to +2.5 kyr older than associated foraminifera (Mollenhauer et al., 2005).

- Evidence from coarse- and fine-fraction $\delta^{18}O$, and ^{230}Th, of drift and non-drift deposits in the Cape Basin suggested sedimentary alkenones had been transported southwards by bottom currents, to a region where the overlying SST is several degrees cooler than that of the source region (Sachs and Anderson, 2003).
- Across a range of global continental shelf/slope settings, Mollenhauer et al. (2008) found that Crenarchaeotal GDGTs have a higher radiocarbon content than that of C_{37} alkenones in the same sediment samples. The younger age of GDGTs suggested more rapid degradation in surface sediments, making them less susceptible to reworking.
- Shah et al. (2008) found GDGT ^{14}C ages were similar to those of foraminifera on the Bermuda Rise, while GDGT ^{14}C ages were older than foraminifera and alkenones in the Santa Monica Basin.
- In a down-core setting in the Panama Basin, paired alkenone and foraminifera ^{14}C ages showed no significant differences (Kusch et al., 2010).

The above studies thus suggest - perhaps with low confidence - that alkenones are more prone to cycles of deposition/resuspension than GDGTs. The contrasting results highlight how redistribution is very site specific.

Unfortunately, similar studies are not available for diatoms (to our knowledge), and although their frustules are siliceous rather than carbon based, ^{14}C dating is possible using carbon in trapped proteins (Hatté et al., 2008).

In the core-top calibrations we rely on reports by the original authors and assume core-tops considered to be affected by reworking have been flagged or excluded from the databases. Similarly, we would exclude SST records at these sites from the synthesis in Part 2. However, we recognise that reworking is not necessarily evident, or may have been stronger in the past, as noted below (Section 3.4).

3.3. Bioturbation

Vertical mixing of near-surface sediments by benthic organisms (bioturbation) potentially affects all marine sediment SST proxies, and results in the smoothing of temperature records at sites with low sedimentation rates (Berger and Heath, 1968; Anderson, 2001; Dolman et al., 2021). The rate (diffusivity) of bioturbation is likely to be greater for small particle sizes (e.g., Wheatcroft, 1992); this could introduce variance between SST records based on different proxies, including those extracted from the same core. Bioturbation can even redistribute foraminifera shells, which are otherwise considered relatively resistant to advection and drift, as demonstrated by age differences of often 1 kyr (exceptionally 3 kyr) between different foraminifera species within the same horizon (Broecker et al., 2006; Mekik, 2014; Ausín et al., 2019). These differences could be significant when using foraminifera as a basis for age models (Part 2) or as benchmarks for evaluating drift susceptibility of other proxies (Section 3.2).

3.4. Past changes in advection and reworking: a motivation for multi-proxy averages

The studies described above help constrain the influences of advection and reworking under modern conditions. What about past climates? Comparison of multiple proxies in down-core paleo reconstructions yields varying levels of consistency in the Southern Ocean (Sicre et al., 2005; Pahnke and Sachs, 2006; Kim et al., 2009; Sikes et al., 2009; dos Santos et al., 2013; De Deckker et al., 2019). Differences in SST reconstructions have sometimes been attributed to stronger lateral advection of alkenones compared to foraminifera or diatoms, during past climates (e.g., Sicre et al., 2005; Kim et al., 2009), but other factors have also been invoked to explain such differences elsewhere, for example different representative depths and/or seasonalities of individual proxies (Pahnke and Sachs, 2006; Sikes et al., 2009; De Deckker et al., 2019). When differences are found, it is often difficult to asses which proxy provides the 'best' estimate. This problem highlights the advantage of averaging across selected proxies in a synthesis of records, to reduce the impact of biases in particular proxies at particular times. The issue provides further motivation for focusing on a Southern Ocean regional mean SST anomaly in Part 2 of this study, rather than carrying out detailed analysis of spatial variability over the Southern Ocean at glacial-interglacial time scales.

4. Seasonality, depth, and habitat tracking

Characteristics of the annual SST cycle under modern conditions are summarised in Fig. S1.1 for reference. The coldest and warmest months are August–September and February–March almost everywhere outside of the Antarctic coastal waters. This homogeneity is an important advantage for our regional calibrations, which should not be degraded by localised seasonal patterns *under modern conditions*. Nevertheless, the representative seasonality (typically "summer" or "annual") of SST proxies is often uncertain in the Southern Ocean because of limited observations (see discussion of each proxy in Section 5) and strong correlation between temperatures in different seasons. For example, if the geochemical index of a particular planktic species is controlled most strongly by spring SST, then a calibration traditionally considered to represent "annual" SST will appear strong only because there is strong correlation between spring SST and annual mean SST in the Southern Ocean (Fig. S1.1). Under past climates, the "annual" SST calibration will only remain valid if the relationship between spring SST and annual mean SST has not changed.

Planktic organisms inhabit a range of depths, depending on species, season and location (Section 5). To reliably reconstruct SST, the recorded temperature signal should be that of the mixed layer, which is very variable across the Southern Ocean. For example, at 40 to 60°S, mixed layer depth tends to increase southwards from 20 to 80 m in summer and from 100 to >300 m in winter (typical values; see Nardelli et al., 2017; Panassa et al., 2018). Given the relatively shallow mixed layer depth in summer, there is a greater likelihood that temperatures recorded by organisms representing summer SST could reflect water temperature in the upper thermocline, as well as in the mixed layer. This adds another source of uncertainty in the reconstructions, since past changes in mixed layer depth (e.g. due to changing stratification or wind stress) could influence the recorded temperature signal.

The prevalence of different species at different water temperatures and depths arises as organisms evolve to thrive under an optimal range of environmental conditions. As climate changes, the season of peak growth could change, or their optimal habitat may shift vertically towards warmer or cooler water: this is known as habitat tracking (e.g., Renaud and Schmidt, 2003; Jonkers and Kučera, 2017). Assuming that a calibration reflects the modern habitat of that species, then habitat tracking can lead to an underestimate of past SST anomalies. For example, if a spring growth peak during interglacials shifts to a summer peak during glacials, then the temperature signal recorded by a geochemical proxy will

change less than that of the climate, simply because the host organism has changed its seasonality (Fig. 2). Habitat tracking is a problem for geochemical proxies but can benefit assemblage based proxies.

In summary, modern calibrations may degrade under past climates because of changes in seasonality, changes in water column structure, and habitat tracking by planktic organisms. We cannot practically correct for these factors, and instead our approach is to assume that each group of organisms shows different responses, such that the errors associated with each group are averaged, to some extent, in a multi-proxy temperature record. While not a perfect solution, it highlights an important benefit of using multiple proxies in SST reconstructions.

5. Calibrations for individual proxies

Here we consider each proxy in turn, with reference to the issues discussed above and to any other specific advantages or disadvantages relevant to the application of each proxy in the Southern Ocean. Further details of the existing calibrations or training datasets are provided in Section S3.

5.1. Alkenones

Long-chain (C_{37}) alkenones are produced by haptophyte algae, mainly *Emiliana huxleyi* and *Gephyrocapsa oceanica*. The relative proportions of the di- and tri-unsaturated alkenones $C_{37:2}$ and $C_{37:3}$ synthesized by these algae vary with water temperature, leading to the widely-used index:

$$U^{K'}_{37} = [C_{37:2}] \Big/ [C_{37:2} + C_{37:3}]. \quad (1)$$

The original index,

$$U^{K}_{37} = [C_{37:2} - C_{37:4}] \Big/ [C_{37:2} + C_{37:3} + C_{37:4}] \quad (2)$$

includes the tetra-unsaturated $C_{37:4}$ alkenone, generally present at lower concentrations than $C_{37:2}$ and $C_{37:3}$ (Brassell et al., 1986; Prahl and Wakeham, 1987; Herbert, 2003; Rama-Corredor et al., 2018). U^{K}_{37} may be relevant in some colder water masses where $C_{37:4}$ is present at higher concentrations (e.g., Bendle and Rosell-Melé, 2004; Martínez-Garcia et al., 2009; Ho et al., 2012; Roberts et al., 2017).

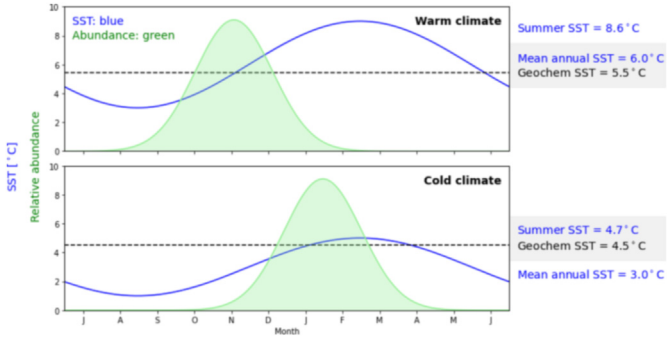

Fig. 2. Simple example of how seasonality could influence SST recorded by geochemical proxies. Abundance of a fictional planktic organism (green shading) peaks 1 month after the SST (blue line) reaches 4 °C. The 'geochemical' SST signal (dashed line) recorded by the organism is the abundance-weighted average SST over 1 year. In the warm climate, the 'geochemical' SST is closer to the mean annual SST, whereas under the cold climate the 'geochemical' SST is closer to the summer (JFM) SST. The difference in SST recorded by the organism (1.0 °C) under these two climates *is smaller than the true differences* in either annual temperature (3.0 °C) or summer temperature (3.9 °C). This illustrates why geochemical calibrations established for modern conditions are not necessarily reliable under past climates. (For interpretation of the references to colour in this figure legend, the reader is referred to the Web version of this article.)

Emiliana huxleyi and *Gephyrocapsa oceanica* are present in the fossil record since c. 290 ka and 1.7 Ma, respectively (Thierstein et al., 1977; Samtleben, 1980; Raffi et al., 2006), indicating that the primary species composition of alkenone synthesisers has likely remained consistent as far back as at least the last two interglacials. In Antarctic coastal waters, iron fertilisation stimulates phytoplankton blooms which include another haptophyte (*Phaeocystis antarctica*) (Alderkamp et al., 2012). These blooms occur in a region well to the south of the currently available SST reconstructions and core-top sediment data, and the contributions of alkenones from *P. antarctica* (which do not necessarily fit the common calibrations) should not be of concern.

5.1.1. Seasonality and depth

Haptophytes are phototrophs and require light. The photic zone can extend below the surface mixed layer and into the thermocline, but alkenone synthesis is considered most productive close to the surface (Müller et al., 1998; Herbert, 2003). This is an important advantage as it limits the potential for vertical habitat tracking (see Section 4). The seasonal pattern of alkenone synthesis remains uncertain in the Southern Ocean (Herbert, 2003; Rosell-Melé and Prahl, 2013; Jaeschke et al., 2017; Nissen et al., 2018), and alkenones are mostly used to reconstruct mean annual SST. At high latitudes where productivity is probably much lower in winter, alkenone synthesis may be more strongly weighted towards summer (Müller et al., 1998; Sikes et al., 1997, 2005, 2005; Jaeschke et al., 2017; Tierney and Tingley, 2018). However, the relationship between $U^{K'}_{37}$ and SST is harder to quantify in these colder waters because the $C_{37:2}$ alkenone concentration is low and the $U^{K'}_{37}$ index approaches zero: here, the original U^{K}_{37} index may be preferable (Martínez-Garcia et al., 2009; Ho et al., 2012; Rosell-Melé and Prahl, 2013).

5.1.2. Non-thermal influences

While temperature is consistently found as the first-order influence on the $U^{K'}_{37}$ index (Prahl et al., 1988, 2010; Müller et al., 1998; Tierney and Tingley, 2018), scatter from the linear calibration arises due to secondary, non-thermal factors. These could include seasonally-variable alkenone export by zooplankton grazing (Conte et al., 2006; Prahl et al., 2006), which modifies the effect of seasonal production noted above; environmental stresses (e.g., light, nutrients: Epstein et al., 1998; Prahl et al., 2006, 2010; Pan and Sun, 2011); and limited but perhaps selective degradation in sediments, which modifies $U^{K'}_{37}$ (Prahl et al., 2010; Pan and Sun, 2011; Rontani et al., 2013). Since we cannot provide a detailed review of these influences here, please see the respective citations for further details. These secondary influences are not (and perhaps cannot be) explicitly corrected for in paleotemperature reconstructions, and their contributions to the scatter in the empirical calibrations introduce associated uncertainties in reconstructed SST. Due to this scatter, typical RMSEPs for $U^{K'}_{37}$ calibrations (Table S3.1) are relatively important in comparison to the magnitude of typical glacial-interglacial SST changes (Part 2). Further, the strengths of these influences (and the degree to which one compensates for another) could have changed under past climates (e.g., Kim et al., 2009; Prahl et al., 2010).

5.1.3. Calibrations relevant to the Southern Ocean

SST is normally considered to vary linearly with $U^{K'}_{37}$, i.e., $T = aU^{K'}_{37} + b$, where a and b are determined empirically (Prahl and

Wakeham, 1987; Prahl et al., 1988; Sikes and Volkman, 1993; Müller et al., 1998; Conte et al., 2006; Tierney and Tingley, 2018). See Table S3.1 for further details. Since by definition $0 \leq U^{K'}_{37} \leq 1$, the temperature range of the index is limited to the range $b \leq T \leq a + b$. Sikes and Volkman (1993) suggested an alternative non-linear calibration $U^{K'}_{37} = 1/[1+\exp(-0.22T+68.6)]$ to capture nonlinearity at low temperatures. The high scatter at low temperatures in their calibration dataset may reflect non-thermal influences or analytical errors as the $C_{37:2}$ concentration becomes very low (Herbert, 2003), and limits the advantage of a nonlinear calibration.

$U^{K'}_{37}$ (which excludes $C_{37:4}$) has generally been preferred over U^{K}_{37} even in the cold Southern Ocean (Sikes et al., 1997; Pahnke and Sachs, 2006; Pelejero et al., 2006). This choice is not universal (Martínez-Garcia et al., 2009; Roberts et al., 2017) and has been questioned: Ho et al. (2012) established strong core-top calibrations for both indices, yet found quite different glacial-interglacial temperature amplitudes in the respective SST reconstructions at site PS75/034−2 in the southeast Pacific. Comparison of U^{K}_{37} versus $U^{K'}_{37}$ merits further attention, but for practical reasons in our synthesis (Part 2) we are restricted to $U^{K'}_{37}$ because there are insufficient available $C_{37:4}$ data to consistently use U^{K}_{37} at all sites.

A global calibration recently established by Tierney and Tingley (2018) using 1344 core-top sediment provided further strong evidence for the general applicability of the linear Prahl et al. (1988) calibration. Regional clusters of positive or negative bias in the SE Pacific and Argentine Basin, reaching ±2 °C, were attributed to lateral advection (Fig. 3 in Tierney and Tingley, 2018), consistent with the discussion in Section 3.1 above. However, other factors - particularly seasonality or reworking - could also contribute (see Sections 3.2 and 5.1.2).

5.1.4. Recommended calibration for the Southern Ocean

As noted above, there is uncertainty regarding what season the alkenone proxy represents at high latitudes (Sikes and Volkman, 1993; Sikes et al., 1997; Rosell-Melé and Prahl, 2013; Nissen et al., 2018). The sediment cores in our study region (see Part 2) have $U^{K'}_{37} < 0.78$, so we use this limit and a northern geographic limit of 23.5°S to assess the relevant calibrations (Fig. 3). Note that we include samples from warmer waters north of 40°S, to ensure warmer interglacial conditions are also represented.

For annual SST reconstructions, the widely-applied Prahl et al. (1988) and almost identical Müller et al. (1998) calibrations provide an excellent fit to the core-top data whether using the selected subset (RMSEP = 1.6 °C) or all Southern Hemisphere data, and are not statistically different from the linear regression line through our subset (Fig. 3a). The greatest difference reaches ~1 °C at low temperatures, supporting the suitability of the Prahl-Müller calibration for annual SST reconstructions in the Southern Ocean, providing the lower limit of the calibration is noted.

In summer, the linear regression line for our selected subset (RMSEP = 1.6 °C) lies between the Müller et al. (1998) and Sikes and Volkman (1993) calibrations (Fig. 3c. Therefore, for summer SST we recommend our new calibration based on the selected subset of the Tierney and Tingley (2018) core-top database.

For both annual and summer reconstructions we find two notable regional clusters of residuals (Fig. 3b,d). A South Atlantic 'cold' cluster lies north of our study region and is not of direct concern for Southern Ocean SST reconstructions. A south-east Pacific 'warm' cluster likely extends to ~ 50°S; alkenone reconstructions from this region may need to be used with caution until the reasons for the warm residuals can be better assessed (e.g., to distinguish between contributions from lateral advection or seasonality/depth).

Although both annual and summer SSTs are well correlated with $U^{K'}_{37}$, we need to remember this could primarily reflect the strong correlation between seasonal temperatures (Fig. S1.1), rather than a direct seasonal response. An argument against using a single index for two seasons is that we lose information on seasonality: the difference between summer and mean annual SST becomes artificially fixed because the two seasons are no longer independent. This prevents meaningful comparison of summer and annual SST changes. However, such a comparison is not possible anyway when only reconstructing one season, and is also of questionable value if using different proxies in different seasons. A second argument against this approach is that fixed seasonal variability introduces artificial bias if the amplitude of the annual temperature cycle has changed in the past. However, fixing the seasonality by using one index for both summer and annual SST does not add any additional bias to what has already been implicitly added by choosing only one season. Therefore, we consider the single index as being suitable for both annual and summer SST reconstructions, using the recommended calibrations, providing this caveat on fixed seasonality is noted.

5.2. Foraminiferal Mg/Ca ratio

Foraminifera inhabit a wide range of depths in the ocean, including the surface and bottom waters. Many species develop calcium carbonate shells, which incorporate trace metals such as magnesium. The shell Mg/Ca ratio depends partly on water temperature-dependent thermodynamic and biological processes during calcification (Mashiotta et al., 1999; Bentov and Erez, 2006; Kunioka et al., 2006), enabling water temperature reconstructions from the Mg/Ca ratio of fossil shells. Foraminifera are heterotrophs, but some planktic species contain algal symbionts (acquired phototrophy: Kimoto, 2015; Stoecker et al., 2009). South of 40°S, the dominant near-surface species are *Globigerinoides bulloides* (mid-latitudes) and *Neogloboquadrina pachyderma* (high latitudes) (Haddam et al., 2016). The deeper-dwelling *Globorotalia inflata* is considered to inhabit the thermocline, and its Mg/Ca ratio may be less representative of the mixed layer (Groeneveld and Chiessi, 2011).

5.2.1. Seasonality and depth

The broad depth habitats of some species, perhaps depending on geographic location or season, lead to uncertainty in the depth and/or season the recorded Mg/Ca temperature represents (Mortyn and Charles, 2003; Jonkers and Kučera, 2015, 2017,; Saenger and Evans, 2019; Tierney et al., 2019). Neither *N. pachyderma* nor *G. bulloides* is associated with an algal symbiont, thus reducing the ecological advantage of inhabiting near-surface waters. *G. bulloides* is associated with a symbiotic cyanobacteria (Bird et al., 2017; Greco et al., 2019) which is less light-dependent than the microalgal symbionts in other planktic foraminifera, perhaps reflecting its host's preference for deeper water (Bird et al., 2017).

Sediment trap data suggest restricted calcification temperature ranges for each species; therefore, if the water temperature lies outside of that range for part of the year, then the calcification temperature may be seasonally biased (Malevich et al., 2019; Tierney et al., 2019). The optimum temperature ranges for *G. bulloides* and *N. pachyderma* are rather wide: approximately 4−29 °C and −1 to 15 °C, respectively (Malevich et al., 2019). Habitat tracking has been reported in several species, but was not considered significant in *G. bulloides* (Jonkers and Kučera, 2017), perhaps reflecting its wide temperature tolerance.

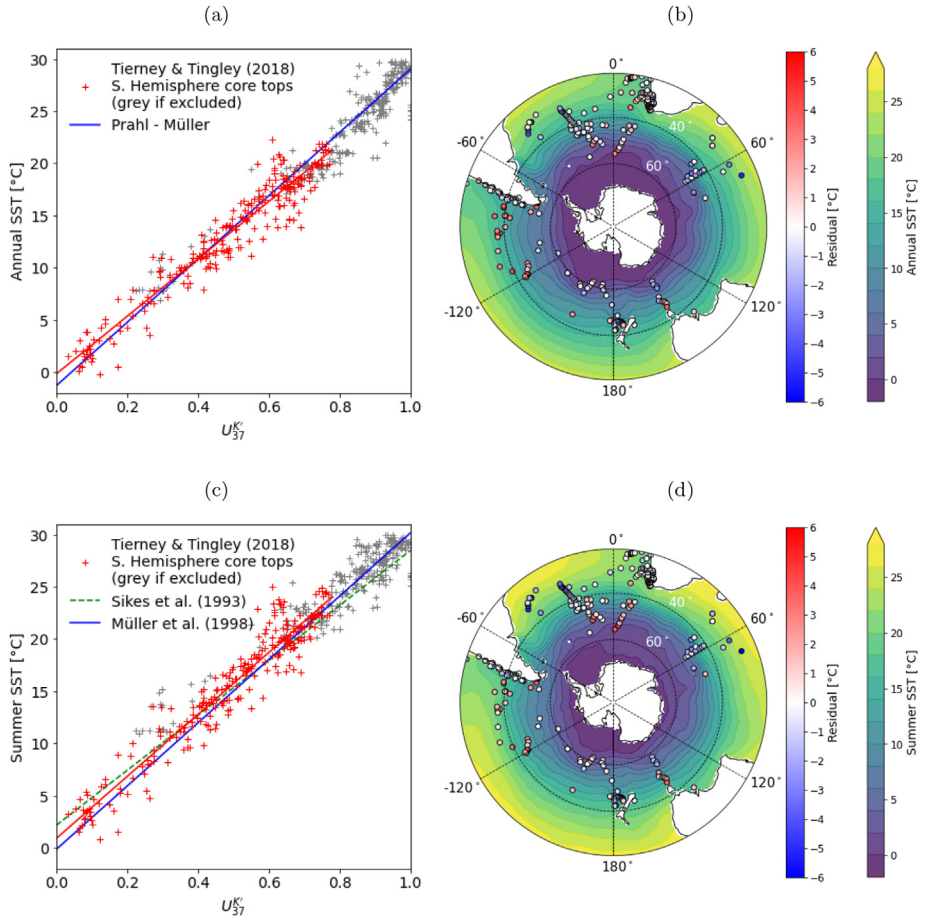

Fig. 3. Left panels (a, c): Southern Hemisphere sites in the Tierney and Tingley (2018) global core-top $U^{K'}_{37}$ database (crosses), with the selected subset (latitude south of 23.5°S and $U^{K'}_{37} < 0.78$: red crosses) and corresponding linear regression (red line); Prahl et al. (1988) and Müller et al. (1998) calibrations (blue line); and Sikes and Volkman (1993) summer calibration (green dashed line). Modern SST is interpolated from the 2018 World Ocean Atlas (WOA2018: Locarnini et al., 2018), in which austral summer is JFM. Right panels (b, d): core-top locations in the selected subset, coloured according to their residuals from the Prahl - Müller calibrations (annual SST) or red regression line (summer SST); shading is the WOA2018 annual or summer SST. (For interpretation of the references to colour in this figure legend, the reader is referred to the Web version of this article.)

5.2.2. Non-thermal influences

Foraminiferal Mg/Ca is influenced by several non-thermal environmental factors, including salinity, carbonate ion concentration and pH, as well as by laboratory analytical procedures (Gray and Evans, 2019; Saenger and Evans, 2019; Tierney et al., 2019). These are summarised here very briefly. Not all species are affected significantly by all factors: for more details, see the recent discussions and corresponding citations in Gray and Evans (2019), Saenger and Evans (2019) and Tierney et al. (2019).

The Mg/Ca distribution is heterogeneous within individual shells (Sadekov et al., 2005; Marr et al., 2011), which could influence point Mg/Ca analysis by LA-ICP-MS. Meanwhile, bulk foraminiferal Mg/Ca (analysed by ICP-AES of dissolved specimens) has been found to vary with shell size in several species commonly used for Mg/Ca paleothermometry (Elderfield et al., 2002; Friedrich et al., 2012). Dependence of Mg/Ca on shell size may arise because Mg/Ca and shell size are both dependent on temperature (or on environmental factors that covary with temperature). Shell size is not readily corrected for in Southern Ocean SST reconstructions because its influence remains uncertain for both relevant species (Elderfield et al., 2002; Friedrich et al., 2012; Saenger and Evans, 2019) and because of variable reporting of shell size data.

Salinity was not an important predictor in recent calibrations based on core-top sediments (Saenger and Evans, 2019; Tierney et al., 2019), but its influence also remains uncertain, due to conflicting reports (Gray and Evans, 2019).

The Mg/Ca proxy assumes steady seawater Ca and Mg concentrations; their long residence times in the oceans (of order Ma: Barrientos et al., 2018) suggests both should only vary slowly at the 100 ka glacial-interglacial time scales, so we can consider both to be constant.

Seawater carbonate chemistry is an important environmental factor, particularly for sediments in deep water (Haddam et al., 2016). Dissolution generally reduces Mg/Ca, thus introducing a cold bias in subsequent temperature reconstructions (Barker et al., 2005; Fehrenbacher and Martin, 2010; Rongstad et al., 2017). However, the rate of dissolution varies widely between sites and species, because of varying water chemistry and the heterogeneous distribution of Mg within foraminifera shells (Bentov and Erez, 2006; Fehrenbacher and Martin, 2010; Rongstad et al., 2017). Regenberg et al. (2014) suggested correcting the Mg/Ca ratio for bottom water carbonate concentration, but for *G. bulloides* this correction yielded little extra skill in SST reconstructions (Saenger and Evans, 2019). Applying such a correction would additionally require reliable estimates of past changes in carbonate chemistry. Instead, we note that relevant Mg/Ca reconstructions in the Southern Ocean (see Part 2) are in water shallower than 3300 m, whereas Haddam et al. (2016) reported significant dissolution only in water deeper than 3800–4200 m in the South Atlantic, Indian and South Pacific ocean basins.

Finally, reductive and non-reductive sample preparation methods remove different amounts of the outer calcite layers, which could bias reconstructed SST depending on the heterogeneity of the Mg distribution within the individual shells (Rosenthal et al., 2004; Sadekov et al., 2005). Here, using the Saenger and Evans (2019) core-top database, we compared *G. bulloides* and *N. pachyderma* samples analysed following both approaches (Fig. 4a). This comparison suggests the Rosenthal et al. (2004) cleaning method correction should be applied in our study region.

5.2.3. Calibrations relevant to the Southern Ocean

Calibrations have been developed for individual species and grouped species (Mashiotta et al., 1999; von Langen et al., 2005; Vázquez Riveiros et al., 2016; Gray and Evans, 2019; Saenger and Evans, 2019; Tierney et al., 2019). See Table S3.2 for more details. Earlier studies may have grouped species together because of limited data, but there are now sufficient data to consider individual species (Mashiotta et al., 1999; von Langen et al., 2005; Vázquez Riveiros et al., 2016; Gray and Evans, 2019; Saenger and Evans, 2019; Tierney et al., 2019). The distinctly higher Mg/Ca in *G. bulloides* than in *N. pachyderma* indicates that temperatures reconstructed with *G. bulloides* would be warmer than those reconstructed with *N. pachyderma* if using a pooled calibration (Fig. 4b).

Saenger and Evans (2019) and Tierney et al. (2019) used temperature-dependent seasonality in their forward models (predicting Mg/Ca from SST and other factors). For example, for *G. bulloides* and *N. pachyderma* Mg/Ca, Saenger and Evans (2019) used 'spring' SST where mean annual SST >10 °C and 'summer' SST otherwise. It is not clear how the seasonality would be applied in reverse when reconstructing SST from Mg/Ca. Does a reconstructed SST of 11 °C represent a mean annual SST under a climate where SST varies annually from 9 to 13 °C, or a summer SST under a climate where SST varies from 6 to 12 °C and has an annual mean of 9 °C? To avoid such ambiguity we should use a calibration where the inverse model (Mg/Ca to SST) is single valued.

Saenger and Evans (2019) and Tierney et al. (2019) both considered several of the non-thermal factors summarised above. To avoid over-fitting, Saenger and Evans (2019) used step-wise regression to construct core-top calibrations including only those parameters which significantly improve the predictive power of the relationship. Tierney et al. (2019) also used a regression-based approach with their core-top data, and then established a Bayesian calibration (BAYMAG) combining core-top data with information from laboratory cultures. Saenger and Evans (2019) found that the optimal calibration for *G. bulloides* was with seasonal temperature and deep water carbonate chemistry, but this was only marginally stronger than their seasonal temperature-only calibration. Tierney et al. (2019) reported the strongest calibration for *G. bulloides* when using seasonal temperature and surface carbonate chemistry, but again achieving little improvement over the univariate temperature-only model. For *N. pachyderma*, Saenger and Evans (2019) found no acceptable calibration while Tierney et al. (2019) achieved reasonable skill with seasonal temperature alone or with seasonal temperature and cleaning method.

5.2.4. Recommended calibration for the Southern Ocean

Constraints on how relevant non-thermal factors have varied in the past are not readily available in our region, and as the uncertainties in these additional factors increase (i.e., as the prior probability density functions become broader), the advantage of the Bayesian approach over a multivariate regression relationship diminishes. In addition, given that the multivariate calibrations discussed above do not greatly improve the predictive skill for either species when compared to the univariate calibrations, the best approach for our particular application, and to ensure consistency between records, is likely to be a univariate calibration. Here we pool the two recent core-top Mg/Ca databases (Saenger and Evans, 2019; Tierney et al., 2019) and remove any sites labelled as 'include = 0' by Tierney et al. (2019). We also apply the Rosenthal et al. (2004) correction for cleaning method.

Starting with *G. bulloides*, and following the approach we used for the alkenones, we first select sites south of the tropics with Mg/Ca < 1.04 mmol/mol (this limit for Mg/Ca matches the range relevant to sediment cores in Part 2). The selected sites represent all three main basins, but are strongly clustered (Fig. 5). Sites in regions identified by Tierney and Tingley (2018) as being problematic in the alkenone core-top calibration, due to strong lateral drift (e.g., the Argentine Basin) are retained here in the Mg/Ca calibration because foraminifera shells are relatively fast sinkers (Section 3).

The selected subset of *G. bulloides* Mg/Ca samples fits the expected logarithmic relationship between SST and Mg/Ca ($r^2 = 0.60$), albeit with wide scatter: core-tops with Mg/Ca of ~1.8 mmol/mol correspond to modern SSTs of ~7 to 17 °C (Fig. 5a). The Vázquez Riveiros et al. (2016), Gray and Evans (2019) and Saenger and Evans (2019) univariate relationships tend to underestimate SST; the Mashiotta et al. (1999) calibration overestimates cool SSTs and underestimates warm SSTs. Note that the Vázquez Riveiros et al. (2016) calibration is for the oxygen isotopic temperature, which more closely represents the calcification temperature. This could include a temperature signal from water beneath the surface mixed layer. Respective RMSEPs for the Mashiotta et al. (1999), Vázquez

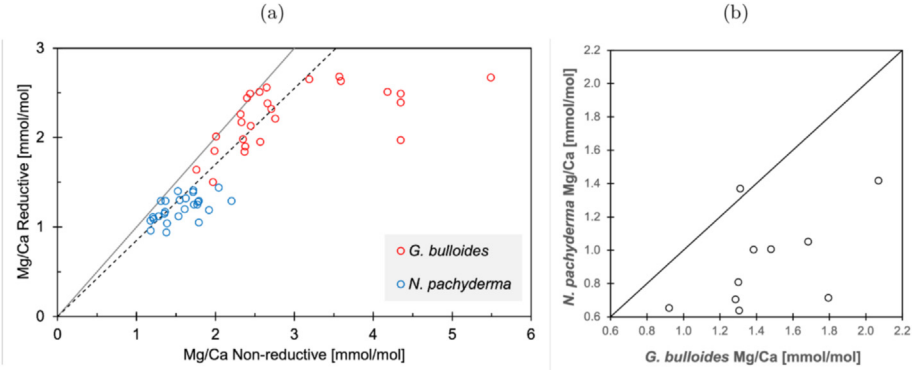

Fig. 4. (a) Comparison of Mg/Ca analysed without vs. with reductive cleaning, using data extracted from the Saenger and Evans (2019) core-top database. The solid line is 1:1 (no difference between methods), and the dashed line corresponds to a 15% reduction in Mg/Ca following reductive cleaning, based on an inter-laboratory comparison by Rosenthal et al. (2004). (b) Mg/Ca in core-tops for which both *G. bulloides* and *N. pachyderma* Mg/Ca have been analysed. Data are from the Tierney et al. (2019) database.

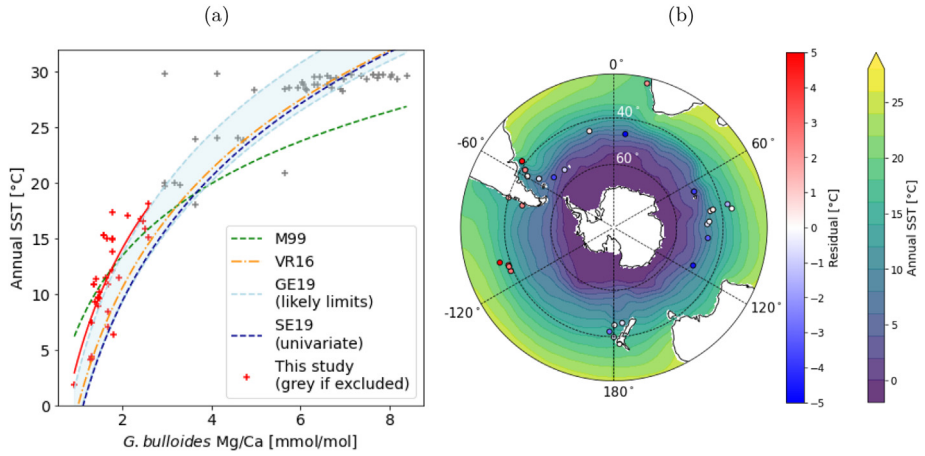

Fig. 5. (a) *G. bulloides* Mg/Ca at Southern Hemisphere sites in the Saenger and Evans (2019) and Tierney et al. (2019) global core-top Mg/Ca database (crosses), with the selected subset (latitude south of 23.5°S and *G. bulloides* Mg/Ca < 2.6 mmol/mol: red crosses) and corresponding regression (red line). Mg/Ca ratios obtained following reductive cleaning were divided by 0.85 (Rosenthal et al., 2004). Modern SST is interpolated from the 2018 World Ocean Atlas (WOA2018: Locarnini et al., 2018). Also plotted are the Mashiotta et al. (1999) calibration (M99, green dashes); Vázquez Riveiros et al. (2016) calibration for oxygen isotopic temperature (VR16, orange dash-dot); Gray and Evans (2019) culture-based calibration (GE19, light blue shading) with the range corresponding to likely limits of surface pH and salinity in the Southern Ocean (8.10–8.25; 32 to 36 psμ, respectively: Jiang et al., 2019); and Saenger and Evans (2019) temperature-only core-top calibration (SE19, dark blue dashes). (b) Core-top locations in the selected subset, coloured according to their residuals from the red regression line in (a); shading is the WOA2018 annual SST. (For interpretation of the references to colour in this figure legend, the reader is referred to the Web version of this article.)

Riveiros et al. (2016), Saenger and Evans (2019) (temperature only), and current best-fit calibrations, using only the selected subset of core tops, are 2.9, 4.6, 5.7 and 2.6 °C, respectively.

The gradient of a logarithmic relationship is steepest at low temperatures, so there is relatively lower sensitivity in our region of interest. Linear regression yields only slightly poorer fit ($r^2 = 0.55$; RMSEP = 2.8 °C). The high scatter likely reflects the importance of non-thermal factors which cannot be readily accounted for in our reconstructions, and although the highest scatter is found outside of our region of interest, the RMSEP for the study region is nearly double that for the alkenones.

Following the same analysis for *N. pachyderma*, we find no significant correlation between SST and Mg/Ca ($r^2 = 0.004$, $p = 0.65$: Fig. 6). The sites around the Antarctic coast form a low-temperature cluster; removing these sites, or using summer SST instead of annual SST, still fails to yield significant correlation. This is consistent with the weak relationships found by Saenger and Evans (2019), even when including additional non-thermal factors. Habitat tracking may be partly responsible for the apparently low temperature sensitivity of Mg/Ca in this species (Jonkers and Kučera, 2015). An alternative is to use the multivariate calibrations established by Tierney et al. (2019). However, this does not solve the problem of habitat tracking, and we would introduce further uncertainties relating to poorly-constrained additional factors, as discussed above.

In summary, given the wide scatter, uncertain influence of non-thermal factors, and poor sensitivity at low temperature, the regional-average *G. bulloides* Mg/Ca SST anomaly might be considered robust (five records were used in our synthesis: see Part 2), while SST anomalies based on individual records are considered unreliable in this region if reconstructed with a univariate relationship. *N. pachyderma* Mg/Ca is considered as an unreliable proxy for SST reconstructions at glacial-interglacial time scales in this region.

5.3. Glycerol dibiphytanyl glycerol tetraethers (GDGTs)

GDGTs are cell-membrane lipids synthesized by many bacteria and archaea, including marine planktic Thaumarchaeota (Schouten et al., 2002). In marine environments, the proportions of specific GDGTs are related to the water temperature in which they were synthesized, and are considered to be stable in marine sediments over long time periods – perhaps tens of millions of years (Schouten et al., 2002; de Bar et al., 2019). The concentrations of three isoprenoidal GDGTs (iGDGTs, numbered 1 to 3, and an isomer of crenarchaeol), each containing 86 carbon atoms but having different structures, were used to define the original TEX_{86} index (Schouten et al., 2002):

$$TEX_{86} = [iGDGT_{2+3+Cren'}]/[iGDGT_{1+2+3+Cren'}] \quad (3)$$

TEX_{86} in global core-top sediment samples has been linearly correlated with SST (Schouten et al., 2002; Kim et al., 2008) but in cold waters (below ~15 °C), the alternative TEX_{86}^{L} index was recommended (Kim et al., 2010):

$$TEX_{86}^{L} = \log_{10}([iGDGT_2]/[iGDGT_{1+2+3}]) \quad (4)$$

Other indices based on hydroxy-GDGTs have also been developed (Huguet et al., 2013; Fietz et al., 2016); see Table S3.3.

In cold polar waters, where the alkenone $U_{37}^{K'}$ index goes to zero and Mg/Ca shows poor temperature sensitivity, or in areas where carbonate dissolution is prevalent, GDGTs may be a promising alternative (Liu et al., 2020). However, other studies focusing on polar regions have found very scattered correlation between SST and TEX_{86} indices (Kim et al., 2010; Shevenell et al., 2011; Ho et al., 2014; Park et al., 2019; Fietz et al., 2020), or inconsistencies with other SST proxies over glacial-interglacial cycles (Fietz et al., 2016).

5.3.1. Seasonality and depth

Observations of GDGTs in suspended particles and sinking particles show strong seasonal variability at some mid to high latitude sites, with a peak export flux in winter/spring (Wuchter et al., 2005), spring/summer (Rodrigo-Gámiz et al., 2015; Park et al., 2019), and no distinct pattern at others (Park et al., 2019). Note that the seasonal pattern of export as measured by sinking particles collected in traps may instead reflect seasonal productivity of larger planktic organisms (e.g., diatoms) rather than GDGT synthesis (Yamamoto et al., 2012; Taylor et al., 2013). Overall, GDGT indices in

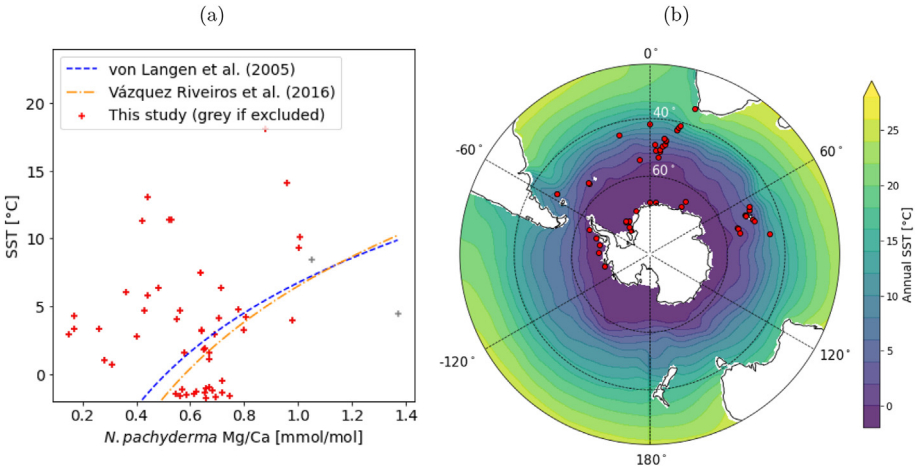

Fig. 6. (a) *N. pachyderma* Mg/Ca at Southern Hemisphere sites in the Saenger and Evans (2019) and Tierney et al. (2019) global core-top Mg/Ca database (crosses), with the selected subset (latitude south of 23.5°S and *N. pachyderma* Mg/Ca < 1.04 mmol/mol) plotted in red). Mg/Ca ratios obtained following reductive cleaning were divided by 0.85 (Rosenthal et al., 2004). Modern SST is interpolated from the 2018 World Ocean Atlas (WOA2018: Locarnini et al., 2018). Also plotted are the von Langen et al. (2005) calibration (blue dashes), and Vázquez Riveiros et al. (2016) calibration for oxygen isotopic temperature (orange dash-dot). (b) Core-top locations in the selected subset; shading is the WOA2018 annual SST. (For interpretation of the references to colour in this figure legend, the reader is referred to the Web version of this article.)

sinking particles appear poorly correlated with seasonal changes in SST and better represent annual mean water temperature (Yamamoto et al., 2012; Rodrigo-Gámiz et al., 2015; Park et al., 2019).

The uncertainty is further enhanced by the poorly constrained distribution of GDGT production in the water column. Sedimentary GDGT indices may best represent a temperature signal integrated over the upper 0 to ~200 m water depth (Kim et al., 2012; Jaeschke et al., 2017; Rodrigo-Gámiz et al., 2015), or perhaps even deeper (Taylor et al., 2013; Hernández-Sánchez et al., 2014; Park et al., 2019; Spencer-Jones et al., 2021), potentially integrating a signal from beneath the surface mixed layer. The sub-surface contribution cannot be accurately quantified in empirical global core-top calibrations with SST, since sub-surface temperature and SST are themselves well correlated at the global scale. However, a deeper contribution would explain some scatter in SST calibrations (noted above), as well as inconsistencies with alkenone SST reconstructions over a wide range of time scales (Fietz et al., 2016; Ho and Laepple, 2016). The lack of a robust, culture-based verification of the empirical GDGT index calibrations is clearly a disadvantage when compared to alkenones.

5.3.2. Non-thermal influences

Marine sediments may contain GDGTs derived from terrestrial fresh water runoff; this contribution can be flagged using the branched versus isoprenoidal tetraether (BIT) index (Weijers et al., 2006; Schouten et al., 2013) and should only be an isolated problem in the Southern Ocean, which is mostly remote from terrestrial runoff sources.

Archaea are abundant well below the mixed layer (e.g., to 500 m: Karner et al., 2001), as noted above, and could make contributions to sedimentary GDGTs that reflect sub-surface conditions. However, Besseling et al. (2020) have argued these deeper communities (comprised of Euryarchaeota rather than Thaumarchaeota) do not synthesise GDGTs, contrary to previous reports (Lincoln et al., 2014). Euryarchaeota can make an additional contribution to sedimentary GDGTs through anaerobic methane oxidation, particularly in sediments (Liu et al., 2011; Taylor et al., 2013); this contribution can be evaluated using the methane index (Zhang et al., 2011) or ring index (see Zhang et al., 2016, for further details).

Further non-thermal influences could arise from diversity within the planktic Thaumarchaeota community (Elling et al., 2015; Qin et al., 2015), growth phase or rate (Elling et al., 2014; Hurley et al., 2016), and dependence on dissolved oxygen concentration (Qin et al., 2015; Hurley et al., 2016). Salinity and pH likely have little influence on GDGT ratios (Elling et al., 2015). Sediment trap data suggested little modification of GDGT ratios as particles sink through the water column (Yamamoto et al., 2012); susceptibility to lateral advection and sediment reworking were discussed in Section 3.

5.3.3. Calibrations relevant to the Southern Ocean

Several calibrations are available for isoprenoidal and hydroxy GDGTs (Schouten et al., 2002; Kim et al., 2010; Shevenell et al., 2011; Tierney and Tingley, 2014; Fietz et al., 2016; Park et al., 2019; Dunkley Jones et al., 2020) (see Table S3.3 for further details). As noted above, linear calibrations for the various indices yield strong scatter in the Southern Ocean (e.g., Kim et al., 2010; Shevenell et al., 2011; Ho et al., 2014; Park et al., 2019).

To overcome this scatter, Tierney and Tingley (2014) proposed a Bayesian calibration, BAYSPAR, where the regression parameters can vary spatially (on a length scale of 20° × 20°). Despite achieving lower residuals without the geographic bias, we do not recommend this method in the Southern Ocean at glacial-interglacial time scales for four reasons.

1. The underlying causes of spatial variability in TEX regression parameters are unknown, and there is then no reason to assume such variability would have remained temporally constant in the past.
2. The reason for a 20° length scale and the control this choice has on reconstructed SSTs are not clear.
3. In areas of the Southern Ocean where core-top data are available, the 90% confidence interval for the predicted SST is generally very wide (typically 7–12 °C), even after applying the spatially variable Bayesian approach to a selected subset of records (see Fig. 7 in Tierney and Tingley, 2014). With a 90% confidence interval, one in ten temperatures are expected to lie outside of even this wide range.
4. Use of spatially-variable regression parameters excludes the reconstruction of SST records obtained from grid boxes which

do not have core-top data: this includes almost the entire Indian Ocean south of 40°S (again, see Fig. 7 in Tierney and Tingley, 2014), where two of four GDGT records covering the last interglacial are located.

GDGT sample analysis by high-performance liquid chromatography - mass spectrometry (HPLC/MS) yields the concentrations of several GDGTs. Using these to define a single index has been criticised because of the inevitable loss of information (Dunkley Jones et al., 2020). Instead, the full assemblage of GDGTs could be used – equivalent to the modern analogue technique employed for species assemblages – with the additional advantage that a linear or exponential relationship does not need to be imposed, in contrast to regression-based (Kim et al., 2010; Fietz et al., 2016) or Bayesian (Tierney and Tingley, 2014) calibrations. However, this potentially promising alternative requires the full assemblage of GDGTs, not just the index, and these are not available at many sites (see Part 2).

5.3.4. Recommended calibration for the Southern Ocean

Here we extract data from the Tierney and Tingley (2014) core-top database, selecting sites south of the tropics with $-0.74 < TEX_{86}^{L} < -0.44$ to match the range relevant to sediment cores (Part 2). We find (as in Tierney and Tingley, 2014) a poor relationship between SST and TEX_{86}^{L} for this region (Fig. 7). The Kim et al. (2010) calibration for TEX_{86}^{L} achieves a reasonable fit above an index of approximately −0.45, but at lower values the linear relationship breaks down, and indices in the range −0.65 to −0.45 (important for the Southern Ocean) have a very weak relationship with SST. This does not improve if removing potentially problematic regions for lateral advection, or if using summer SST: sensitivity still remains very poor at indices below −0.45. The non-thermal influences on GDGTs are currently poorly constrained in the Southern Ocean (see Section 5.3.2) and likely contribute to the wide scatter. We also note the uncertain depth and seasonality of GDGT production in the water column. Therefore, we chose not to use the TEX_{86}^{L} index in our glacial-interglacial SST reconstructions in the Southern Ocean (Part 2). However, the advantages of GDGTs noted at the start of Section 5.3, and the possibility to apply the modern analogue technique to the full suite of GDGTs, indicate the great potential this method could have in this region once the non-thermal influences are better understood.

5.4. Diatom assemblages

Diatoms are a group of algae inhabiting a diverse range of aquatic environments, including the photic zone of the ocean. Due to their large total biomass, diatoms play an important role in the global carbon cycle, likely influencing changes in atmospheric CO_2 over glacial-interglacial time scales (Martin, 1990; Lafond et al., 2020). Diatom cell walls ('frustules') are silicon-based rather than carbonate-based and remain preserved in areas subject to carbonate dissolution, where foraminiferal proxy records are not available. However, diatoms are instead subject to silica dissolution (see below). Diatom species diversity is greater than that of foraminifera at high latitudes, which is advantageous where foraminiferal assemblages become almost mono-specific (and thus insensitive to SST) in water colder than ~2° (e.g. Haddam et al., 2016).

5.4.1. Seasonality and depth

Diatom production is widely reported as peaking in spring and summer, often characterised as short, intense blooms with considerable inter-annual variability (typically Nov to Feb: Abelmann and Gersonde, 1991; Fischer et al., 2002; Closset et al., 2015; Rembauville et al., 2015; Rigual-Hernández et al., 2016). However, blooms are not evident everywhere, and some studies have reported long, broad abundance peaks through spring and summer, with time-varying dominance of different species (Rigual-Hernández et al., 2016; Eriksen et al., 2018). Selective dissolution of particular species can skew the preserved sedimentary assemblage towards a spring-dominated signal in some areas (subantarctic zone) and summer-dominated signal in others (Antarctic zone, polar frontal zone) (Rigual-Hernández et al., 2016). Overall, assemblages preserved in sediments could potentially reflect many direct and indirect environmental factors, and accumulation over many years will likely reflect conditions across several seasons. This is particularly the case at high latitudes, where species associated with sea ice will contribute a winter sea ice signal into the assemblage, even though the seasonal productivity of that species is weighted towards spring (Crosta et al., 2005). Despite these influences across multiple seasons, diatom census counts are used as a proxy for summer SST rather than annual SST. However, we

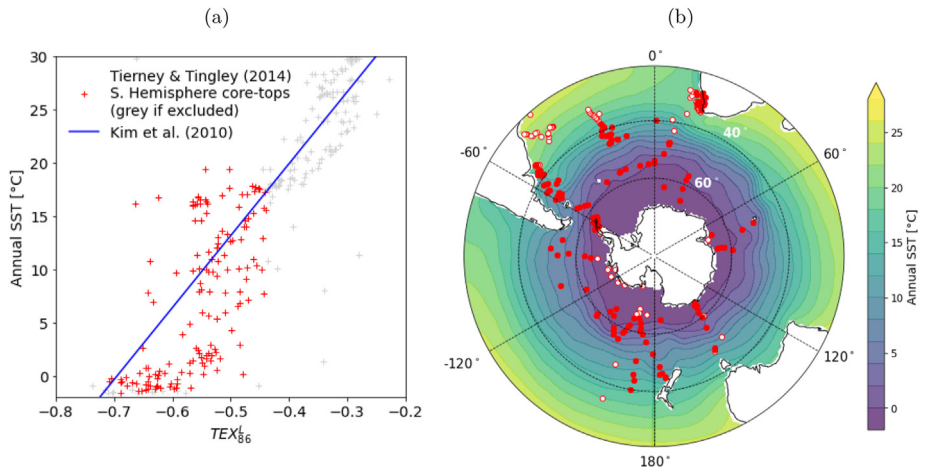

Fig. 7. (a): TEX_{86}^{L} at Southern Hemisphere sites in the Tierney and Tingley (2014) global core-top database (crosses), with the selected subset (latitude south of 23.5°S and $-0.74 < TEX_{86}^{L} < -0.44$) plotted in red. Modern SST is interpolated from the 2018 World Ocean Atlas (WOA2018: Locarnini et al., 2018). Also plotted is the Kim et al. (2010) calibration (blue line). (b): Core-top locations in the selected subset; sites in red or white are included in or excluded from the selected subset. (For interpretation of the references to colour in this figure legend, the reader is referred to the Web version of this article.)

should bear in mind that the *productivity* and the *sedimentary assemblage* do not necessarily share the same environmental controls or seasonal interpretation.

Marine diatoms are phototrophs, and in-situ water sampling has indeed shown peak diatom abundances in the uppermost ~100 m at 35 to 60°S (Wright et al., 2010; Schlüter et al., 2011; Nunes et al., 2019; Lafond et al., 2020). However, this depth range likely extends beneath the relatively shallow summer mixed layer (Section 2). In addition, diatoms actively modify their buoyancy and travel between the mixed layer, thermocline and even deeper layers depending on their other needs besides light, such as nutrient availability (Smetacek, 1985; Raven and Waite, 2004). This is important because some aspects of the diatom life cycle likely occur below the mixed layer or even the photic zone, implying their growth over a full life cycle could depend on conditions at multiple depths in the water column.

5.4.2. Non-thermal influences

Diatom census counts are used to reconstruct sea-ice duration as well as SST. Armand et al. (2005), Crosta et al. (2005) and Romero et al. (2005) studied temperature and sea ice influences on three groups of diatoms (sea-ice related, open ocean, and tropical/subtropical) (Table S3.4). Taxa in the sea-ice related group showed little diversity in their temperature sensitivity, but showed varying responses to sea-ice cover or duration. Therefore, those taxa would be less suitable for SST reconstructions because variance in their assemblage mainly reflects sea ice conditions, not SST. However, taxa in the other two subsets (open ocean and tropical/subtropical) showed more diverse SST responses, and assemblages of these taxa were considered sensitive to SST.

Nutrients limit diatom productivity in many parts of the Southern Ocean (e.g., Martin, 1990; Boyd, 2002; Quéguiner, 2013; Lafond et al., 2020). However, Fe fertilisation results in localised regions of high diatom abundance (blooms) down-wind of terrestrial dust sources, and is the basis of the "Iron Hypothesis" describing the role of diatoms in glacial-interglacial CO_2 changes (Martin, 1990). Nutrient-rich runoff from the Antarctic ice sheet also promotes diatom blooms (Alderkamp et al., 2012; Death et al., 2014). Fe-fertilised assemblages may be distinct from those in Fe-limited surface waters (Assmy et al., 2007; Armand et al., 2008; Lafond et al., 2020), thus presenting the possibility of different assemblages in waters with the same SST. This is not necessarily a problem for the MAT, providing that the training dataset contains a sufficient number of samples of both environments – indeed, the ability to cope with non-unique temperature relationships is one of the advantages of the MAT. However, it would be a problem if the species assemblage associated with Fe fertilisation is not sensitive to SST, since close analogues could be selected which contain little temperature information. A further problem arises if advection/dispersion becomes important, since the 'Fe fertilisation' assemblage could be mixed with the temperature-sensitive 'Fe limited' assemblage to varying amounts downstream of the Fe source.

Grazing by zooplankton modifies the surface and sedimentary diatom assemblages (Abelmann and Gersonde, 1991; Granĺi et al., 1993; Smetacek et al., 2004). These studies show grazing can be very localised, but we assume such variance is smoothed out over the time scales represented by core-top and down-core sediment samples. Nevertheless, long-term changes in the characteristics of species-selective grazing could still alter the remaining assemblage. Overall, the complex dependence of diatom populations on nutrients and grazing cannot be considered in detail here and instead we highlight this as a reason why considering a regional average over multiple proxies is more appropriate than detailed interpretation of a small number of records.

Silica dissolution affects diatoms as they are sinking, as well as on the sea floor. Dissolution can strongly skew the sedimentary diatom assemblage, but the rate depends on several physical and biological factors including species and water temperature (Zielinski et al., 1998; Passow et al., 2011; Rigual-Hernández et al., 2016). The net effect is that a few robust species can dominate the assemblage, after the dissolution of species with less resistant shells (Zielinski et al., 1998). The extent to which dissolution influence Southern Ocean SST reconstructions warrants consideration in more detail in future.

Finally, we re-iterate the potentially important influence of advection on diatom reconstructions (Section 3): not only because the provenance of local sedimentary temperature signal may be hundreds of km away, but (perhaps more importantly) because species-dependent sinking rates in aggregates or faecal pellets could result in lateral advection modifying the sedimentary assemblage. This potentially important source of error has not been quantified for diatoms.

5.4.3. Recommendations for the Southern Ocean

Diatom responses to SST and other environmental factors were studied in detail by Armand et al. (2005), Crosta et al. (2005) and Romero et al. (2005), and more recently by Esper and Gersonde (2014). In these studies, diatom assemblages are primarily distinguished by their geographic location and are considered (from south to north) as the Southern Antarctic zone, Northern Antarctic zone, and Subantarctic zone (Table S3.4). Esper and Gersonde (2014) compared several reconstruction techniques (transfer function, MAT, weighted average, weighted average – partial least squares) and different configurations thereof. Applying these to Southern Ocean cores PS1768-8 and PS58/271 (both MIS 6 to present) yielded very similar results.

Publicly available data are currently limited for diatom reconstructions, both for the core-top databases and the for sediment cores used in Part 2. This prevents a detailed evaluation of this proxy or calculation of SSTs in the way we have done for the others. However, differences between reconstruction methods appear relatively small (Esper and Gersonde, 2014), and in Part 2 we use the original SST reconstructions, noting that each is well represented by the SST-dependent groups listed in Table S3.4. However, nutrients, dissolution and advection could all have important influences on sedimentary diatom assemblages at glacial/interglacial time scales, and for this reason we would recommend a cautious approach to detailed interpretation of individual SST reconstructions from diatoms in this region at present.

5.5. Dinoflagellate cyst (dinocyst) assemblages

Dinoflagellates are a group of phototrophic and heterotrophic planktic organisms. Some dinoflagellates produce resting cysts (hereafter referred to as dinocysts) during their reproductive phase, which can be preserved in marine sediments (e.g., Marret et al., 2001). Dinocysts are relatively diverse even in cold waters, where foraminifera assemblages lose environmental sensitivity. The organic walls of dinocysts are also considered to represent a significant advantage over the other assemblage-based proxies (diatoms, foraminifera, radiolarians) which suffer from dissolution in some environments (Esper and Zonneveld, 2007). Nevertheless, dinocysts are instead subject to oxidation in some locations.

5.5.1. Seasonality and depth

Phototrophic dinoflagellates inhabit the photic zone, and observations show peak abundances in the upper 100 m (Fiala et al., 1998; Wright et al., 2010; Schlüter et al., 2011; Nunes et al., 2019). Heterotrophic dinoflagellates are free from this restriction of light availability, but their primary food source is diatoms which are also

near-surface dwellers. The timing of peak heterotrophic dinoflagellates abundance is closely tied to the peak in their phytoplankton food source (e.g., Kjæret et al., 2000).

In the Southern Ocean, dinocysts have been used to reconstruct summer and winter SST (Marret et al., 2001) or just summer SST (Esper and Zonneveld, 2007). However, seasonality data are sparse. East of New Zealand, sediment traps yielded a spring peak at a subtropical site and a much broader peak at a subpolar site (Prebble et al., 2013). The Southern Ocean Time Series (SOTS) Observatory south of Australia (at ~47°S) showed a broad peak in abundance, with an amplitude reaching ~100 times the winter abundance, lasting from November until at least April (Eriksen et al., 2018). These data suggest that both summer and annual temperature reconstructions could be robust, although similarly to diatoms we note again that the seasonal influences on *abundance* and *assemblage* are not necessarily the same.

5.5.2. Non-thermal influences

Besides SST, dinocyst assemblages are strongly influenced by several environmental factors including nutrients, salinity and sea ice, as well as proximity to coastline (De Vernal et al., 1997; Esper and Zonneveld, 2007; Verleye and Louwye, 2010; Prebble et al., 2013). While it is an advantage if multiple environmental factors can be reconstructed simultaneously, this introduces considerable additional uncertainty unless sufficiently large training datasets are available. Wide diversity in assemblages has been reported between sites with similar SST, along gradients in other environmental factors (Verleye and Louwye, 2010; Prebble et al., 2013). This is not necessarily a problem for the MAT, which is non-parametric and can reconstruct relationships that are not single-valued; however, it imposes high demands on the training dataset, as core-top samples will need to thoroughly represent a wide range of environmental conditions to avoid no-analogue or 'ambiguous' reconstructions. In this respect, regional datasets could be more appropriate (Prebble et al., 2013). Rapid zonal transport in the Southern Ocean should dampen such regional variance in our study area, albeit at the cost of advection-related problems. Careful selection of taxa is also required, to exclude those taxa showing little temperature response (Marret et al., 2001; Esper and Zonneveld, 2007).

Some dinocyst species are degraded by oxygenated bottom waters, leading to a distinction between degradation-sensitive 'S-cysts' and degradation-resistant 'R-cysts' (see Table 2 in Esper and Zonneveld, 2007). Species-dependent degradation modifies the sedimentary assemblage (Versteegh and Zonneveld, 2002) and is quantified using the '*kt*' index, so that high *kt* index samples can be rejected (Zonneveld et al., 2007). The calculation for *kt* assumes a fixed initial ratio of S-cysts to R-cysts, on the basis of sediment trap and core-top data from just two warm regions (Arabian Sea and Namibia shelf) (Zonneveld et al., 2007). Since R-cysts tend to be phototrophic, while S-cysts tend to be heterotrophic (Zonneveld et al., 2007), then the initial populations of S-cysts and R-cysts in the Southern Ocean will likely have very different environmental drivers, and it seems very unlikely that their ratio is either spatially or temporally constant, suggesting that the *kt* index is not necessarily a reliable indicator of degradation in this region.

Finally, dinocysts are relatively slow sinkers (see Section 3 and Nooteboom et al., 2019), leading to potentially large temperature errors in some regions. Very limited data have indicated quite different near-surface and sedimentary dinocyst assemblages (Prebble et al., 2013), although the causes of this difference remain unclear.

5.5.3. Recommendations for the Southern Ocean

The two studies applying dinocyst assemblages in our region used their own databases (Marret et al., 2001; Zonneveld et al., 2007); see Table S3.5 for further details. Marret et al. (2001) compiled a training dataset with core-tops from all sectors of the Southern Ocean (south of 38°S), but focused around New Zealand and Tasmania. Their database includes few samples from warm regions, and there is a risk that interglacial conditions at mid-latitudes may be poorly represented: fewer than 10 sites have a summer SST >17 °C (see Fig. 5 in Marret et al., 2001). Furthermore, given the potential influence of non-thermal factors, and the corresponding need for a large training dataset, then 81 sites is rather limited for assemblages with 39 selected taxa.

Esper and Zonneveld (2007) employed a larger core-top dataset (but still with only 138 sites) for their South Atlantic SST reconstructions, with a greater representation of warm sites than Marret et al. (2001). Esper and Zonneveld (2007) excluded core-top and down-core samples with $kt > 10$, although in our region we question the validity of this index without adequate sediment trap data from the mid- and high-latitudes (see above). Esper and Zonneveld (2007) encountered two important problems. First was low total abundances in sediment cores, for example fewer than 100 cysts in 37 of 52 down-core samples at site PS1768-8 and in 16 of 56 samples at PS2082-1, affecting over half the LIG samples at both sites. Secondly, no-analogue conditions in the penultimate glacial were attributed to the high relative abundances (72–93%) of *Nematosphaeropsis labyrinthus* cysts, which did not match any modern core-top samples. While this was simply overcome by excluding these samples, it raises concerns regarding the temporal stability of this group in terms of their apparent environmental influences. If these training data are not representative of conditions in the penultimate glacial, are temperatures reconstructed in other periods still reliable, even if close analogues are available? Is the assemblage sensitive to some other ecological factor that changes with time? In a newer and much larger core-top database (Zonneveld et al., 2013), *N. labyrinthus* abundances exceed 70% at only 3 out of 332 extra-tropical sites in the Southern Hemisphere, so employing the newer, larger dataset will not solve this problem.

Applying the MAT to the Zonneveld et al. (2013) dataset, but including only the temperature-sensitive taxa selected by Esper and Zonneveld (2007), and including only sites south of the tropics, yields RMSEPs for annual and summer SST of 2.2 °C and 2.3 °C in our study region (see Fig. 8 and Table S3.5 for more details). There is good geographic coverage in the S. Atlantic and SW Pacific, the two regions where reconstructions are available in Part 2. Nevertheless, some important limitations of this approach are as follows.

1. The open-ocean sites in this database are somewhat clustered (Fig. 8), potentially over-estimating the strength of the reconstruction if several analogues are selected from a tight cluster (Section 2).
2. We know that assemblages may be affected by oxidation of some taxa, but do not yet know if the *kt* index for oxidation is reliable in our study region.
3. There is evidence for regional bias (clusters of warm or cold residuals), for example a warm cluster south-east of New Zealand and a cold cluster in the Indian Ocean (Fig. 8). These could indicate advection bias. However, residuals appear well mixed in many areas.
4. The high abundance of *N. labyrinthus* during the penultimate glacial at site PS2082-1 has no modern analogue, suggestive of some other important but unknown factor influencing the assemblage.

Owing to these specific problems, and the prospect of considerable advection bias (Section 3), we chose not to include the

Table 2
Summary of the recommended calibrations, and advantages and disadvantages of SST proxies applied to the Southern Ocean for paleoclimate reconstructions at glacial-interglacial time scales.

Proxy and recommendation	Advantages	Disadvantages	RMSEP south of **40**°S
Alkenones Annual SST: Prahl-Müller $T = 30.3U^{K'}_{37} - 1.30$ Summer SST: This study $T = 29.7U^{K'}_{37} + 0.90$	Robust, global calibration. Alkenones preserved where siliceous/carbonate fossils have dissolved. Alkenones synthesized in photic zone, thus reducing depth uncertainty and limiting potential for habitat tracking.	Limited range of index: low SST sensitivity in polar waters. Uncertain seasonality at high latitudes; could have changed under past climates. Regional clustering of residuals indicates some advection bias (possibly from sediment reworking).	Annual 1.6 °C Summer 1.7 °C
Foraminiferal Mg/Ca *G. bulloides* annual SST: $T = 13.0\ln(1.23\mathrm{Mg/Ca})$ *N. pachyderma*: Not recommended in Southern Ocean	Foraminifera are fast sinkers (low advection bias). Open-ended calibration not implicitly limited at low temperatures.	Post-depositional dissolution may introduce uncertain bias in reconstructed temperature. Low number of core-top samples available south of the tropics (weak calibration). Uncertain influences of non-thermal factors, particularly carbonate chemistry. Uncertain what season or depth the temperature represents. *N. pachyderma* Mg/Ca very weakly temperature dependent in study region.	*G. bull.* Annual 2.6 °C N. pachy. N/A
GDGTs Not recommended yet for glacial-interglacial SST reconstructions in the Southern Ocean.	GDGTs preserved where siliceous/carbonate fossils have dissolved. GDGTs synthesized in photic zone, thus reducing depth uncertainty and limiting potential for habitat tracking. Potential to use modern analogue technique with full GDGTs assemblage, rather than parametric calibration with single index.	Very weak calibration for TEX_{86} indices in Southern Ocean. Poorly constrained seasonality and depth. Poor coverage of core-top samples in mid-latitudes.	N/A
Diatoms assemblage Use summer SST in original publications	Suitable for high latitudes where alkenones, Mg/Ca, and foraminifera assemblage lose sensitivity. Weak influence of reconstruction method.	Assemblage skewed by silica dissolution. Representative depth and season poorly known (can spend part of life cycle below photic zone). Poorly constrained advection bias: individuals sink slowly; groups sink quickly, may be species-dependent. Lack of publicly available training dataset.	See original publications.
Dinocysts assemblage Not recommended yet for glacial-interglacial SST reconstructions in the Southern Ocean.	Good potential for high latitudes where alkenones, Mg/Ca and foraminifera assemblage lose sensitivity.	Insufficient and clustered training data at present. Species-dependent oxidation not well quantified in the Southern Ocean. Available sediment cores often have low counts or non-analogue conditions. Slow sinkers subject to considerable advection bias.	Annual 2.2 °C Summer 2.3 °C (likely to be optimistic)
Foraminifera assemblage Annual and summer: Modern analogue technique as described in Section 5.6.	Lowest RMSEP of all tested proxies. No regions of notably cold or warm residuals. Fast sinkers (low advection bias). Multiple seasons can be reconstructed without the fixed seasonality imposed in the alkenones annual/summer reconstructions.	Inconsistent reporting of taxa hinders comparison of records and consistent reconstruction method. Carbonate dissolution may skew assemblage in deep water. Assemblage becomes monospecific and loses sensitivity in water colder than ~1 °C.	Annual 1.2 °C Summer 1.4 °C
Radiolarians assemblage Not recommended in the Southern Ocean, due to the potential influence of advection.	Diverse assemblage even in cold water.	Likely susceptible to species-dependent advection and/or re-working (Section 3). Insufficient/inconsistent training data for whole Southern Ocean.	N/A

dinocyst reconstructions in our synthesis (Part 2). However, the reasonable performance of the MAT at Southern Ocean sites in the Zonneveld et al. (2013) core-top database (Fig. 8) suggests dinocysts could be a reliable SST proxy in the Southern Ocean if these problems can be overcome.

5.6. Foraminifera assemblages

Foraminifera assemblages are the most commonly used proxy for SST reconstructions in the Southern Ocean, representing about half of the records selected in Part 2. Some general information on foraminifera was provided above for Mg/Ca (Section 5.2). Here we provide additional information relevant to reconstructions using the assemblage rather than the individual species.

5.6.1. Seasonality and depth

Assessment of what season(s) the assemblage represents is difficult for foraminifera in the Southern Ocean. Comparison of the limited available regional sediment trap data with global datasets suggests that seasonal patterns in the Northern Hemisphere high latitudes (for which far more data are available) are not necessarily replicated in the Southern Hemisphere (Jonkers and Kučera, 2015). Few species have published seasonality data (Table S3.6). As well as varying geographically, seasonality can vary markedly between different years at the same site (e.g., Donner and Wefer, 1994; King and Howard, 2005; Bergami et al., 2009). Some studies have used summer peaks in plankton fluxes as the basis for assuming the foraminifera assemblage best represents summer SST (e.g., Becquey and Gersonde, 2003). However, the sedimentary assemblage is represented as percentages, not absolute abundances, in the MAT. Even if the individual abundance of a particular species (i.e., the count per m^3 or per m^2 in the water column) is strongly seasonal, its percentage abundance in a census count of sedimentary foraminifera deposited over many years will also depend on the abundances of other species, which may have different seasonal characteristics containing signals from multiple seasons.

Similarly to seasonality, little direct evidence is available with which to constrain the representative depths of most planktic

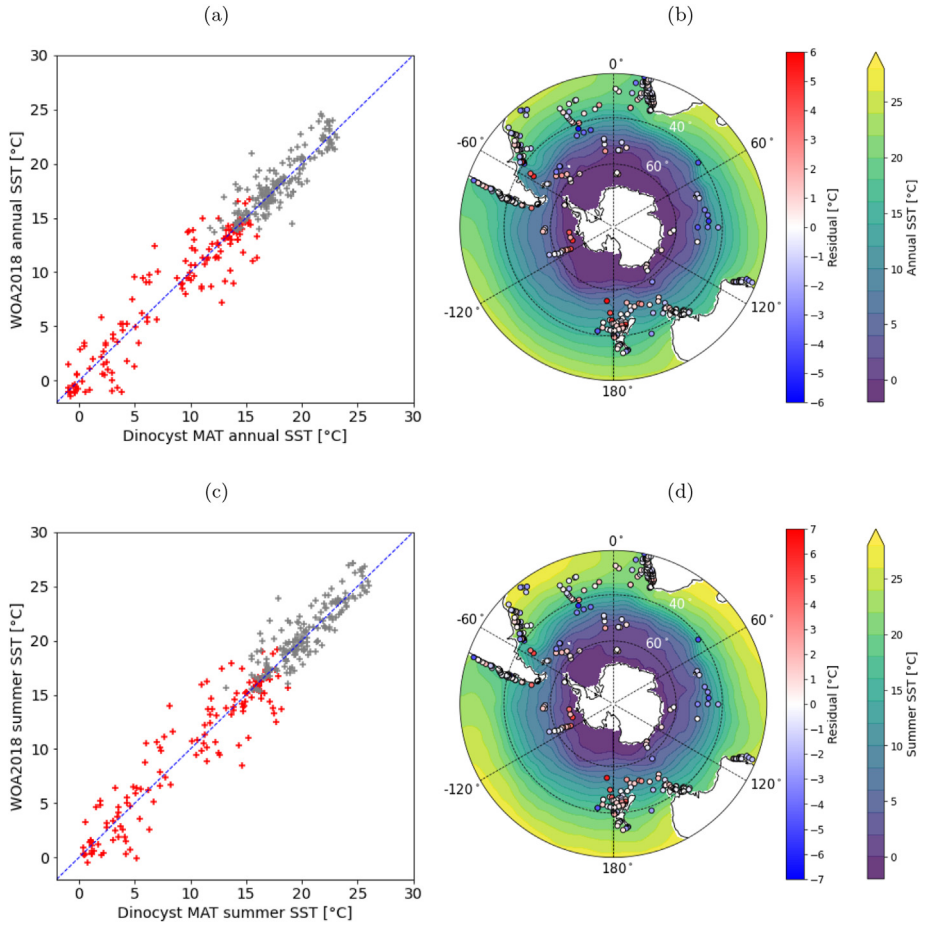

Fig. 8. Left panels (a, c): SST reconstructions at Southern Hemisphere sites in the Zonneveld et al. (2013) global core-top dinocyst database (crosses), with the sites south of 40°S plotted in red. Here, SST at each site in the database is reconstructed in a leave-one-out analysis by the modern analogue technique (MAT) using the unweighted mean of the 5 closest analogues. Modern SST is interpolated from the 2018 World Ocean Atlas (WOA2018: Locarnini et al., 2018), in which austral summer is JFM. Right panels (b, d): core-top locations, coloured according to the temperature difference between the reconstructed and WOA2018 SST; shading is the WOA2018 annual or summer SST. (For interpretation of the references to colour in this figure legend, the reader is referred to the Web version of this article.)

foraminifera species in the Southern Ocean. As noted above (Section 5.2), *G. bulloides* appears to be consistently near-surface (upper 100 m); *N. pachyderma* is more variable (but still within the upper 200 m); and insufficient observations are available to constrain depths of other species in the Southern Ocean (Mortyn and Charles, 2003; King and Howard, 2005; Bergami et al., 2009). Unlike Mg/Ca, where the calcification depth is critical in reconstructions (Section 5.2), the depth habitat of each individual species in an assemblage may be less important. For example, the abundance of a species that inhabits depths below the mixed layer may still depend on surface temperature-dependent factors, such as the productivity of surface-dwelling prey species, even though its representative Mg/Ca temperature might better reflect the sub-surface temperature.

As the number of species increases, interpreting the representative seasonality and depth of a full census count quickly becomes very complex. In practice we have to rely on an empirical calibration with a chosen seasonal SST and accept that past changes in seasonality or depth could result in uncertainties that cannot be easily quantified.

5.6.2. Non-thermal influences

Abundances could be influenced by many factors besides water temperature, such as food availability and predation (Fraile et al., 2008; Meilland et al., 2016; Lessa et al., 2020). However, some of these factors may themselves co-vary with SST, and describing the details of all of these controls is outside the scope of this study (and generally not well constrained in the Southern Ocean). Application of the MAT with the large core-top database will hopefully sample a sufficiently wide range of conditions that the reconstruction remains robust during past climates.

As noted for the other foraminifera-based proxies, post-depositional carbonate dissolution is potentially a significant source of bias in SST reconstructions (Niebler and Gersonde, 1998; Haddam et al., 2016). Dissolution initially removes species with smaller and more delicate shells, eventually skewing the overall abundances (Haddam et al., 2016). For this reason, Haddam et al. (2016) assessed at what depths carbonate dissolution is likely to become significant, through analysis of core-top assemblage changes with ocean depth in their database. They recommend excluding records below 3800 m in the South Pacific and South Indian oceans, and 4200 m in the South Atlantic.

Foraminifera are considered as the least susceptible to advection of the proxies considered here. This is supported by the lack of regional clusters of residuals in core-top reconstructions using the MAT (see below).

5.6.3. Recommendations for the Southern Ocean

Records published using this proxy span over 30 years, with diverse training datasets, reference SSTs, reconstruction techniques, inferred seasonality, and choice of taxa (too numerous to

describe here; see for example Howard and Prell, 1992; Becquey and Gersonde, 2003; Barrows and Juggins, 2005; Schaefer et al., 2005; Hayward et al., 2012; Cortese et al., 2013; Haddam et al., 2016). This presents a challenge for comparing records or even for calculating a meaningful regional average temperature anomaly. A recent database of 598 core-top foraminifera assemblages (Haddam et al., 2016) combines three databases used in many of the earlier Southern Ocean SST reconstructions (Salvinac, 1998; Kučera et al., 2005; Cortese et al., 2013) and allows sediment core records to be reanalysed using a common approach. Haddam et al. (2016) applied some quality-control and inclusion criteria: 15°S to 64°S; water depth between 500 and the maximum noted above; fragment sizes >150 μm. The database contains 35 taxa, with some grouping necessary for consistency between the contributing databases.

Choices of taxa and reconstruction technique are ultimately subjective and dependent on application, so here we focus on our Southern Ocean SST synthesis (Part 2) as an example. Given the very varied approaches used in existing reconstructions, we attempt to re-calculate SST at as many sites as possible using a consistent method. In the MAT we need to choose which taxa to include, the number of closest analogues (k), and how to average over these k closest analogues (e.g., mean, median, weighted average). These choices are made based on leave-one-out analysis of the complete dataset. In this method, SST at each of the N sites in the database is reconstructed using the remaining $N-1$ sites. This gives N pairs of modern ocean atlas SST and reconstructed SST with which to estimate the RMSEP.

Not all of the taxa in the Haddam et al. (2016) database are reported in all the marine sediment core assemblages (Part 2), and not all taxa show clear temperature dependence (Fig. 9). Using only the taxa common to the 14 sediment cores used in Part 2 maximises consistency, but restricts the choice to just *G. bulloides*, *G. inflata* and *N. pachyderma*. These three species alone still yield surprisingly reasonable accuracy (RMSEP 2.1 °C for annual SST south of 40°S). However, none of those three species is abundant in warm water (Fig. 9), which may limit accuracy during interglacials.

The chosen subset of taxa (shaded blue in Fig. 9) is a compromise between inclusivity and consistency, acknowledging that we will not use exactly the same subset for each reconstruction. We also exclude some deeper-dwelling *globoratalia* species which degrade the SST reconstructions. For the 13 selected taxa, the RMSEP at sites south of 40°S reaches a broad minimum at 1.2 °C with $k = 7$ to 12 (annual) or 1.4 °C with $k = 4$ to 15 (summer). For those records missing some of the selected taxa, the RMSEP will be slightly higher: between 1.2 and 2.1 °C for the annual SST. The geographic distribution of the residuals (Fig. 10b) shows that positive and negative residuals do not generally form regional clusters (compare with Figs. 3 and 5 for Mg/Ca and alkenones). This suggests that regional influences, e.g. due to drift, do not make an important contribution to the reconstruction. This is the only proxy we have analysed which does not show such regional clustering of residuals.

Overall we consider the foraminifera assemblage to be the most reliable of the seven proxies, for Southern Ocean SST reconstructions at glacial-interglacial time scales. However, we note that the representative seasonality and depth of reconstructed temperatures are not well constrained, potentially introducing errors if seasonality or water column structure were markedly different under past climates.

5.7. Radiolarian assemblages

Radiolarians are a group of marine zooplankton, with mostly siliceous shells, distributed throughout the world's oceans including the Southern Ocean and Antarctic coastal waters (e.g, Nishimura and Nakaseko, 2011; Boltovskoy and Correa, 2016). Similar to foraminifera, radiolarians sometimes show acquired phototrophy (Stoecker et al., 2009). This group's species diversity in cold polar waters, and their siliceous shells, provide similar advantages to those of diatoms and dinocysts when compared to the more widely used foraminifera assemblages.

As noted in Section 3 above, lateral drift is a potentially major problem for radiolarian-based SST reconstructions in the Southern Ocean. Not only are most radiolarians relatively slow sinkers (perhaps travelling some hundreds of km between their surface habitat and eventual deposition in ocean sediments), but their sinking rates vary widely across several important radiolarian taxa in the Southern Ocean Takahashi and Honjo (1983) (Fig. 1). This is significant because lateral advection can then modify the assemblage itself, further compounding what is already a difficult issue regarding the non-local temperature signal in local sediments. Since we would use an empirical core-top reconstruction technique such as the MAT or transfer functions, the effects of this advection will be compensated for, to some extent, in a training dataset evaluated by the 'leave-one-out' approach. Indeed, an RMSEP <2 °C can be achieved for radiolarian training datasets relevant to the Southern Ocean (Cortese and Abelmann, 2002; Cortese and Prebble, 2015). The real problem arises in the reconstructions, since the training dataset may no longer be relevant if advection patterns have changed in the past. Bearing in mind it is the assemblage as well as the provenance that is being modified, then correcting for advection is neither practical nor robust in a temperature reconstruction. The problem can also become circular if an advection correction is applied based on paleo-currents when the paleo-currents themselves are dependent on climate models optimised using an ocean temperature reconstruction.

Two additional problems with applying radiolarian assemblages in the SST synthesis (Part 2) are the lack of a recent training dataset covering all of the Southern Ocean (Table S3.7), and very variable reporting of taxa in the available radiolarian counts. Several core-top databases have been compiled (Table S3.7), with varying geographic coverage and taxa (CLIMAP Project Members, 1976; Cortese and Abelmann, 2002; Hernández-Almeida et al., 2020). To apply the MAT, the optimal choices are a detailed Pacific database of 429 taxa – albeit with significant gaps (Hernández-Almeida et al., 2020), or the much older CLIMAP Project Members (1976) database covering all three basins but with only 22 taxa. The CLIMAP Project Members (1976) database includes insufficient data from warm water, having only 4 sites with summer SST >20 °C, thus reducing the confidence in reconstruction of warmer interglacial conditions. We can combine the two databases, but then encounter problems matching taxa (there have been many changes in the taxonomy over the last 40 years), and after some necessary grouping we find only 18 taxa are common to both databases. With this combined database, there are still relatively few subtropical sites.

5.7.1. Recommendations for the Southern Ocean

Even before reviewing additional non-thermal influences, we consider it likely that the species-dependent lateral advection will prevent reliable application of radiolarian assemblages as an SST proxy in the Southern Ocean, at least until detailed analysis of the resulting errors has been carried out using high-resolution dispersion modelling under both modern and a range of paleo-ocean circulation patterns. We note again that back-trajectory modelling will not necessarily solve this problem, since the 'advection' includes a dispersion component (related to the Southern Ocean eddy diffusivity) that cannot necessarily be corrected by back-trajectory modelling (Batchelder, 2006). Therefore,

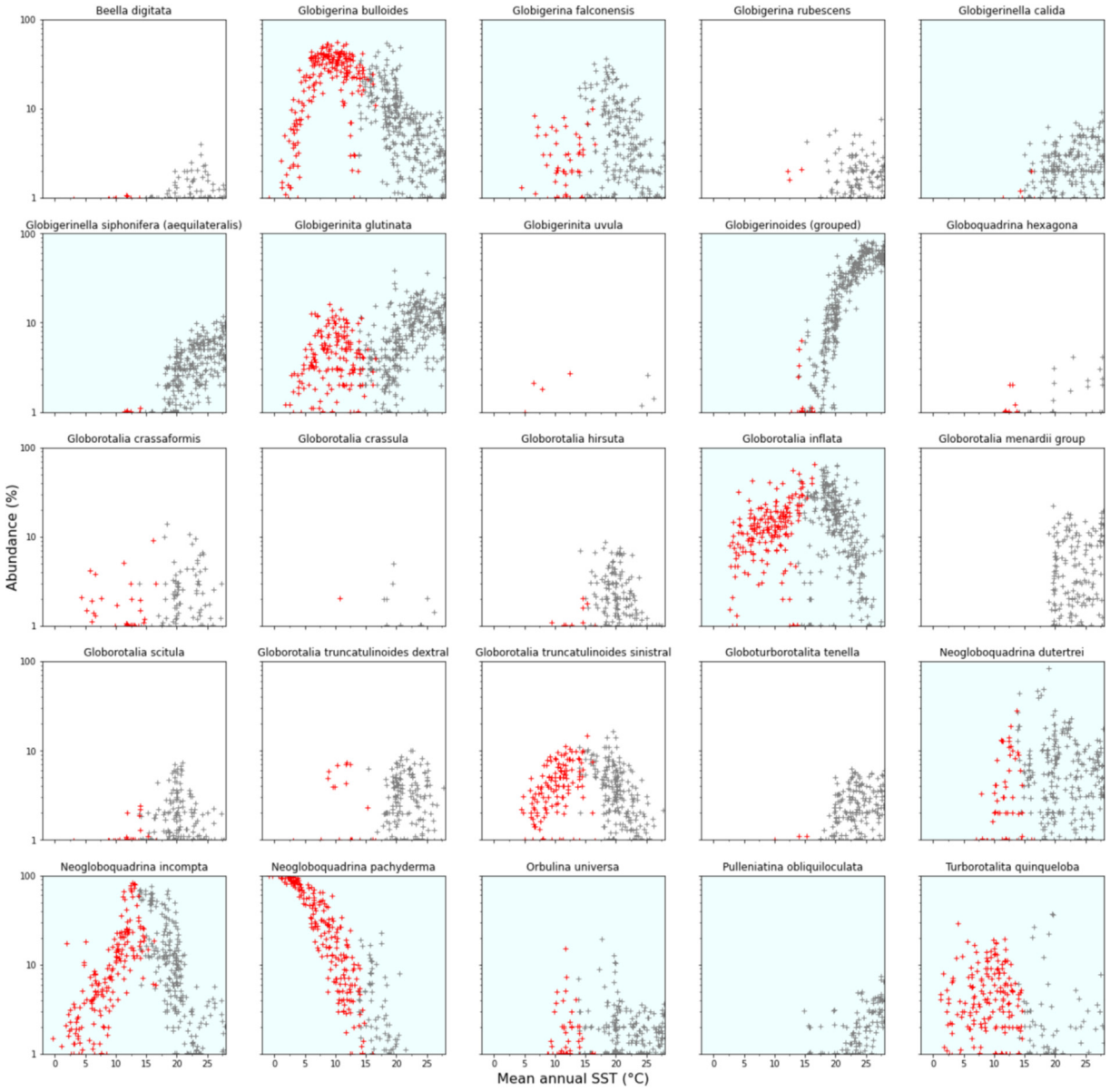

Fig. 9. Temperature dependence of principal Southern Ocean foraminifera in the Haddam et al. (2016) core-top database. Modern mean annual SST at each site is interpolated from the 2018 World Ocean Atlas (WOA2018: Locarnini et al., 2018). Sites south of 40°S are plotted in red, the remainder (15–40°S) are grey. Blue shading indicates taxa selected for the MAT in the Southern Ocean. The increasing abundance of some taxa (e.g., *G. calida* and *G. siphonifera*) in water just slightly warmer than that encountered south of 40°S, shows the importance of including these warm water taxa in the reconstructions even if they are not abundant in the study region under modern conditions – this will allow us to reliably reconstruct SST under warmer climates. Equivalent plots for summer and winter seasons (not shown) are very similar. Note that some taxa in the Haddam et al. (2016) database have been grouped here (e.g., *Globigerinoides*), to better match taxa reported in the sediment core assemblages available in Part 2. (For interpretation of the references to colour in this figure legend, the reader is referred to the Web version of this article.)

we have chosen not to include this proxy in the synthesis in Part 2.

6. Discussion and conclusions

The previous sections have reviewed many potential issues relevant to SST reconstructions in the Southern Ocean, leading to the recommendations summarised in Table 2. Three significant problems in this region are lateral advection, poorly constrained seasonality or depth, and important non-thermal influences. These are unlikely to be realistically corrected for in SST reconstructions, without adding considerable additional uncertainties, especially considering that their influence may have varied under past climates. All proxies suffer from at least one of these three problems, but foraminifera assemblages are considered the most reliable overall, as reflected by their relatively low RMSEP (annual and summer 1.2 °C and 1.4 °C), fast sinking rates (Fig. 1), and lack of regional clusters of warm/cold residuals (Fig. 10b). Alkenones were considered as the most reliable geochemical proxy, but could be susceptible to lateral advection and sediment reworking in some regions (Section 5.1). In addition, changes in the seasonality of alkenone synthesis are uncertain under past climates (Fig. 2). Both proxies lose sensitivity in cold polar waters (SST <1–2 °C), but it is possible this restriction could be alleviated for alkenones by wider use of $C_{37:4}$.

G. bulloides Mg/Ca and diatom assemblages were considered as moderately reliable when analysing a regional average rather than

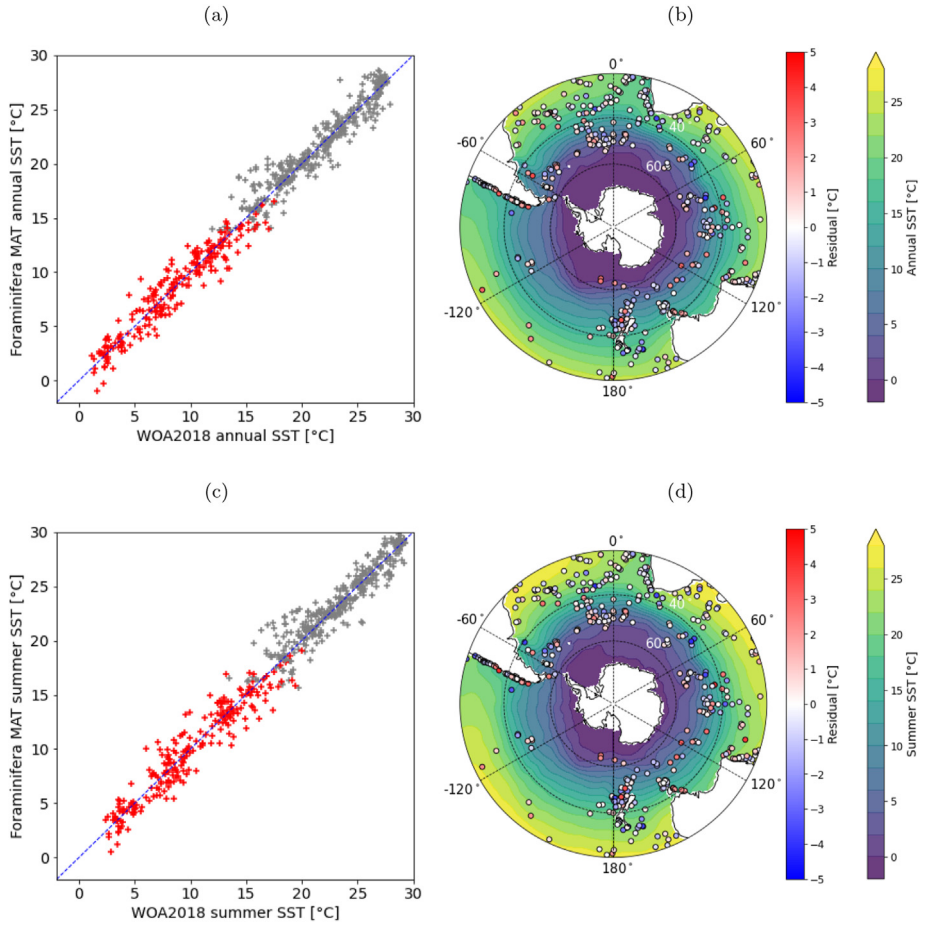

Fig. 10. Left panels (a, c): SST reconstructions at Southern Hemisphere sites in the Haddam et al. (2016) global core-top foraminifera database (crosses), with the sites south of 40°S plotted in red. Here, SST at each site in the database is reconstructed in a leave-one-out analysis by the modern analogue technique (MAT), using the taxa highlighted in Fig. 9 and the unweighted mean of the 7 closest analogues. Modern SST is interpolated from the 2018 World Ocean Atlas (WOA2018: Locarnini et al., 2018), in which austral summer is JFM. Right panels (b, d): core-top locations, coloured according to the temperature difference between the reconstructed and WOA2018 SST; shading is the WOA2018 annual or summer SST. (For interpretation of the references to colour in this figure legend, the reader is referred to the Web version of this article.)

individual sites (see advantages and disadvantages in Table 2). Both are potentially subject to important non-thermal influences, and diatom assemblages may be modified by species-selective advection (Section 3). However, diatoms are particularly valuable at higher latitudes where alkenones and foraminifera lose sensitivity, and in these areas they may be more reliable than the alternatives.

Finally the *N. pachyderma* Mg/Ca, GDGTs, dinocyst assemblages and radiolarian assemblages were considered unreliable in the Southern Ocean for reconstructions at glacial-interglacial time scales. The former two have very weak calibrations, and the latter two are likely to be strongly susceptible to advection, amongst other drawbacks (Table 2).

By selecting alkenones, *G. bulloides* Mg/Ca, foraminifera assemblages, and diatom assemblages we are not only choosing the proxies we consider to be most reliable, but fortuitously we are also sampling important diversity: the set includes two geochemical proxies based on one phototrophic group and one heterotrophic group, and two assemblages also based on one phototrophic group and one heterotrophic group. This diverse mix reduces sensitivity of *regional average SST reconstructions* to poorly-constrained past changes in nutrients, population dynamics, seasonality or other environmental factors that likely affect one group more than another. The set includes two proxies that are not sensitive to carbonate dissolution, which leads to poor preservation of foraminifera (for either SST reconstructions or age modelling) in some regions of the Southern Ocean (e.g., Xiao et al., 2016).

These recommendations apply to Southern Ocean SST reconstructions for the purposes of calculating a regional SST anomaly. Even the proxies considered as most reliable may still be susceptible to significant and poorly constrained errors in particular regions. For that reason we would be very cautious when analysing spatial variability, a small number of sites, or a single proxy type.

Author contributions

DC carried out the data analysis. Both authors contributed to writing the paper.

Declaration of competing interest

The authors declare that they have no known competing financial interests or personal relationships that could have appeared to influence the work reported in this paper.

Acknowledgements

This study was funded by the European Union's Horizon 2020 research and innovation programme under grant agreement no. 820575 (TiPACCs). We gratefully acknowledge the many authors of

the original temperature reconstructions and core-top sediment datasets, who have made their data available for use in this study. We acknowledge the developers of the open-source Python packages which we used for data analysis. Finally, we thank an anonymous reviewer for their valuable comments.

Appendix A. Supplementary data

Supplementary data to this article can be found online at https://doi.org/10.1016/j.quascirev.2021.107191.

References

Abelmann, A., Gersonde, R., 1991. Biosiliceous particle flux in the Southern Ocean. Mar. Chem. 35 (1), 503–536.

Alderkamp, A.-C., Mills, M.M., van Dijken, G.L., Laan, P., Thuróczy, C.-E., Gerringa, L.J.A., de Baar, H.J.W., Payne, C.D., Visser, R.J.W., Buma, A.G.J., Arrigo, K.R., 2012. Iron from melting glaciers fuels phytoplankton blooms in the Amundsen Sea (Southern Ocean): phytoplankton characteristics and productivity. Deep Sea Res. Part II 71–76, 32–48.

Alldredge, A.L., Gotschalk, C.C., 1989. Direct observations of the mass flocculation of diatom blooms: characteristics, settling velocities and formation of diatom aggregates. Deep Sea Res. Part A 36 (2), 159–171.

Anderson, D.M., 2001. Attenuation of millennial-scale events by bioturbation in marine sediments. Paleoceanography 16 (4), 352–357.

Anderson, D.M., Lively, J.J., Reardon, E.M., Price, C.A., 1985. Sinking characteristics of dinoflagellate cysts1. Limnol. Oceanogr. 30 (5), 1000–1009.

Armand, L.K., Crosta, X., Quéguiner, B., Mosseri, J., Garcia, N., 2008. Diatoms preserved in surface sediments of the northeastern Kerguelen Plateau. Deep Sea Res. Part II 55 (5), 677–692.

Armand, L.K., Crosta, X., Romero, O., Pichon, J.-J., 2005. The biogeography of major diatom taxa in Southern Ocean sediments: 1. Sea ice related species. Palaeogeogr. Palaeoclimatol. Palaeoecol. 223 (1), 93–126.

Ashjian, C.J., Gallager, S.M., Plourde, S., 2005. Transport of plankton and particles between the chukchi and beaufort seas during summer 2002, described using a video plankton recorder. Deep Sea Res. Part II 52 (24), 3259–3280.

Assmy, P., Henjes, J., Klaas, C., Smetacek, V., 2007. Mechanisms determining species dominance in a phytoplankton bloom induced by the iron fertilization experiment EisenEx in the Southern Ocean. Deep Sea Res. Part I 54 (3), 340–362.

Ausín, B., Haghipour, N., Wacker, L., Voelker, A.H.L., Hodell, D., Magill, C., Looser, N., Bernasconi, S.M., Eglinton, T.I., 2019. Radiocarbon age offsets between two surface dwelling planktonic foraminifera species during abrupt climate events in the SW iberian margin. Paleoceanogr. Paleoclimatol. 34 (1), 63–78.

Barker, S., Cacho, I., Benway, H., Tachikawa, K., 2005. Planktonic foraminiferal Mg/Ca as a proxy for past oceanic temperatures: a methodological overview and data compilation for the Last Glacial Maximum. Quat. Sci. Rev. 24 (7), 821–834.

Barrientos, N., Lear, C.H., Jakobsson, M., Stranne, C., O'Regan, M., Cronin, T.M., Gukov, A.Y., Coxall, H.K., 2018. Arctic Ocean benthic foraminifera Mg/Ca ratios and global Mg/Ca-temperature calibrations: new constraints at low temperatures. Geochem. Cosmochim. Acta 236, 240–259.

Barrows, T.T., Juggins, S., 2005. Sea-surface temperatures around the Australian margin and Indian ocean during the last glacial maximum. Quat. Sci. Rev. 24 (7), 1017–1047.

Batchelder, H.P., 2006. Forward-in-Time-/Backward-in-Time-Trajectory (FITT/BITT) modeling of particles and organisms in the coastal ocean. J. Atmos. Ocean. Technol. 23 (5), 727–741.

Becquey, S., Gersonde, R., 2003. A 0.55-Ma paleotemperature record from the subantarctic zone: implications for antarctic circumpolar current development. Paleoceanography 18 (1), 1014.

Belcher, A., Manno, C., Ward, P., Henson, S.A., Sanders, R., Tarling, G.A., 2017. Copepod faecal pellet transfer through the meso- and bathypelagic layers in the Southern Ocean in spring. Biogeosciences 14 (6), 1511–1525.

Bendle, J., Rosell-Melé, A., 2004. Distributions of UK37 and UK37′ in the surface waters and sediments of the Nordic Seas: implications for paleoceanography. G-cubed 5 (11).

Benthien, A., Müller, P.J., 2000. Anomalously low alkenone temperatures caused by lateral particle and sediment transport in the Malvinas Current region, western Argentine Basin. Deep Sea Res. Part I 47 (12), 2369–2393.

Bentov, S., Erez, J., 2006. Impact of biomineralization processes on the Mg content of foraminiferal shells: a biological perspective. G-cubed 7 (1), Q01P08.

Bergami, C., Capotondi, L., Langone, L., Giglio, F., Ravaioli, M., 2009. Distribution of living planktonic foraminifera in the ross Sea and the pacific sector of the Southern Ocean (Antarctica). Mar. Micropaleontol. 73 (1), 37–48.

Berger, W.H., Heath, G.R., 1968. Vertical mixing in pelagic sediments. J. Mar. Res. 26 (2), 134–143.

Besseling, M.A., Hopmans, E.C., Bale, N.J., Schouten, S., Damsté, J.S.S., Villanueva, L., 2020. The absence of intact polar lipid-derived GDGTs in marine waters dominated by Marine Group II: implications for lipid biosynthesis in Archaea - scientific Reports. Sci. Rep. 10 (294), 1–10.

Bintanja, R., van Oldenborgh, G.J., Katsman, C.A., 2015. The effect of increased fresh water from Antarctic ice shelves on future trends in Antarctic sea ice. Ann. Glaciol. 56 (69), 120–126.

Bird, C., Darling, K.F., Russell, A.D., Davis, C.V., Fehrenbacher, J., Free, A., Wyman, M., Ngwenya, B.T., 2017. Cyanobacterial endobionts within a major marine planktonic calcifier (*Globigerina bulloides*, Foraminifera) revealed by 16S rRNA metabarcoding. Biogeosciences 14 (4), 901–920.

Boltovskoy, D., Correa, N., 2016. Biogeography of radiolaria polycystina (protista) in the World Ocean. Prog. Oceanogr. 149, 82–105.

Boyd, P.W., 2002. Environmental factors controlling phytoplankton processes in the Southern Ocean. J. Phycol. 38 (5), 844–861.

Brassell, S.C., Eglinton, G., Marlowe, I.T., Pflaumann, U., Sarnthein, M., 1986. Molecular stratigraphy: a new tool for climatic assessment. Nature 320 (6058), 129–133.

Broecker, W., Barker, S., Clark, E., Hajdas, I., Bonani, G., 2006. Anomalous radiocarbon ages for foraminifera shells. Paleoceanography 21 (2).

Capron, E., Govin, A., Stone, E.J., Masson-Delmotte, V., Mulitza, S., Otto-Bliesner, B., Rasmussen, T.L., Sime, L.C., Waelbroeck, C., Wolff, E.W., 2014. Temporal and spatial structure of multi-millennial temperature changes at high latitudes during the Last Interglacial. Quat. Sci. Rev. 103, 116–133.

Caromel, A.G.M., Schmidt, D.N., Phillips, J.C., Rayfield, E.J., 2014. Hydrodynamic constraints on the evolution and ecology of planktic foraminifera. Mar. Micropaleontol. 106, 69–78.

Chandler, D., Langebroek, P., 2021. Southern Ocean sea surface temperature synthesis: Part 2. Penultimate glacial and last interglacial. Quat. Sci. Rev. 271, 107190.

CLIMAP Project Members, 1976. The surface of the ice-age earth. Science 191 (4232), 1131–1137.

Closset, I., Cardinal, D., Bray, S.G., Thil, F., Djouraev, I., Rigual-Hernández, A.S., Trull, T.W., 2015. Seasonal variations, origin, and fate of settling diatoms in the Southern Ocean tracked by silicon isotope records in deep sediment traps. Global Biogeochem. Cycles 29 (9), 1495–1510.

Conte, M.H., Sicre, M.-A., Rühlemann, C., Weber, J.C., Schulte, S., Schulz-Bull, D., Blanz, T., 2006. Global temperature calibration of the alkenone unsaturation index (UK'37) in surface waters and comparison with surface sediments. G-cubed 7 (2).

Cortese, G., Abelmann, A., 2002. Radiolarian-based paleotemperatures during the last 160 kyr at ODP site 1089 (Southern Ocean, atlantic sector). Palaeogeogr. Palaeoclimatol. Palaeoecol. 182 (3), 259–286.

Cortese, G., Dunbar, G.B., Carter, L., Scott, G., Bostock, H., Bowen, M., Crundwell, M., Hayward, B.W., Howard, W., Martínez, J.I., Moy, A., Neil, H., Sabaa, A., Sturm, A., 2013. Southwest Pacific Ocean response to a warmer world: insights from Marine Isotope Stage 5e. Paleoceanography 28 (3), 585–598.

Cortese, G., Prebble, J., 2015. A radiolarian-based modern analogue dataset for palaeoenvironmental reconstructions in the southwest Pacific. Mar. Micropaleontol. 118, 34–49.

Crosta, X., Romero, O., Armand, L.K., Pichon, J.-J., 2005. The biogeography of major diatom taxa in Southern Ocean sediments: 2. Open ocean related species. Palaeogeogr. Palaeoclimatol. Palaeoecol. 223 (1), 66–92.

de Bar, M.W., Rampen, S.W., Hopmans, E.C., Sinninghe Damsté, J.S., Schouten, S., 2019. Constraining the applicability of organic paleotemperature proxies for the last 90 Myrs. Org. Geochem. 128, 122–136.

De Deckker, P., Barrows, T.T., Stuut, J.-B.W., van der Kaars, S., Ayress, M.A., Rogers, J., Chaproniere, G., 2019. Land–sea correlations in the Australian region: 460ka of changes recorded in a deep-sea core offshore Tasmania. Part 2: the marine compared with the terrestrial record. Aust. J. Earth Sci. 66 (1), 17–36.

De Vernal, A., Rochon, A., Turon, J.-L., Matthiessen, J., 1997. Organic-walled dinoflagellate cysts: palynological tracers of sea-surface conditions in middle to high latitude marine environments. Geobios 30 (7), 905–920.

Death, R., Wadham, J.L., Monteiro, F., Le Brocq, A.M., Tranter, M., Ridgwell, A., Dutkiewicz, S., Raiswell, R., 2014. Antarctic ice sheet fertilises the Southern Ocean. Biogeosciences 11 (10), 2635–2643.

DeConto, R.M., Pollard, D., Alley, R.B., Velicogna, I., Gasson, E., Gomez, N., Sadai, S., Condron, A., Gilford, D.M., Ashe, E.L., Kopp, R.E., Li, D., Dutton, A., 2021. The Paris Climate Agreement and future sea-level rise from Antarctica. Nature 593 (7857), 83–89.

Dezileau, L., Bareille, G., Reyss, J.L., Lemoine, F., 2000. Evidence for strong sediment redistribution by bottom currents along the southeast Indian ridge. Deep Sea Res. Part I 47 (10), 1899–1936.

Dolman, A.M., Groeneveld, J., Mollenhauer, G., Ho, S.L., Laepple, T., 2021. Estimating bioturbation from replicated small-sample radiocarbon ages. Paleoceanogr. Paleoclimatol. 36 (7), e2020PA004142.

Donner, B., Wefer, G., 1994. Flux and stable isotope composition of Neogloboquadrina pachyderma and other planktonic foraminifers in the Southern Ocean (Atlantic sector). Deep Sea Res. Part I 41 (11), 1733–1743.

dos Santos, R.A.L., Spooner, M.I., Barrows, T.T., De Deckker, P., Damsté, J.S.S., Schouten, S., 2013. Comparison of organic (UK'37, TEXH86, LDI) and faunal proxies (foraminiferal assemblages) for reconstruction of late Quaternary sea surface temperature variability from offshore southeastern Australia. Paleoceanography 28 (3), 377–387.

Dunkley Jones, T., Eley, Y.L., Thomson, W., Greene, S.E., Mandel, I., Edgar, K., Bendle, J.A., 2020. OPTiMAL: a new machine learning approach for GDGT-based palaeothermometry. Clim. Past 16 (6), 2599–2617.

Dutton, A., Carlson, A.E., Long, A.J., Milne, G.A., Clark, P.U., DeConto, R., Horton, B.P., Rahmstorf, S., Raymo, M.E., 2015. Sea-level rise due to polar ice-sheet mass loss during past warm periods. Science 349 (6244), aaa4019.

Elderfield, H., Vautravers, M., Cooper, M., 2002. The relationship between shell size

and Mg/Ca, Sr/Ca, δ18O, and δ13C of species of planktonic foraminifera. G-cubed 3 (8), 1–13.
Elling, F.J., Könneke, M., Lipp, J.S., Becker, K.W., Gagen, E.J., Hinrichs, K.-U., 2014. Effects of growth phase on the membrane lipid composition of the thaumarchaeon Nitrosopumilus maritimus and their implications for archaeal lipid distributions in the marine environment. Geochem. Cosmochim. Acta 141, 579–597.
Elling, F.J., Könneke, M., Mußmann, M., Greve, A., Hinrichs, K.-U., 2015. Influence of temperature, pH, and salinity on membrane lipid composition and TEX86 of marine planktonic thaumarchaeal isolates. Geochem. Cosmochim. Acta 171, 238–255.
Eppley, R.W., Holmes, R.W., Strickland, J.D.H., 1967. Sinking rates of marine phytoplankton measured with a fluorometer. J. Exp. Mar. Biol. Ecol. 1 (2), 191–208.
Epstein, B.L., D'Hondt, S., Quinn, J.G., Zhang, J., Hargraves, P.E., 1998. An effect of dissolved nutrient concentrations on alkenone-based temperature estimates. Paleoceanography 13 (2), 122–126.
Eriksen, R., Trull, T.W., Davies, D., Jansen, P., Davidson, A.T., Westwood, K., van den Enden, R., 2018. Seasonal succession of phytoplankton community structure from autonomous sampling at the Australian Southern Ocean Time Series (SOTS) observatory. Mar. Ecol. Prog. Ser. 589, 13–31.
Esper, O., Gersonde, R., 2014. Quaternary surface water temperature estimations: new diatom transfer functions for the Southern Ocean. Palaeogeogr. Palaeoclimatol. Palaeoecol. 414, 1–19.
Esper, O., Zonneveld, K.A.F., 2007. The potential of organic-walled dinoflagellate cysts for the reconstruction of past sea-surface conditions in the Southern Ocean. Mar. Micropaleontol. 65 (3), 185–212.
Fehrenbacher, J., Martin, P., 2010. Mg/Ca variability of the planktonic foraminifera G. ruber s.s. and N. dutertrei from shallow and deep cores determined by electron microprobe image mapping. IOP Conf. Ser. Earth Environ. Sci. 9 (1), 012018.
Fiala, M., Semeneh, M., Oriol, L., 1998. Size-fractionated phytoplankton biomass and species composition in the Indian sector of the Southern Ocean during austral summer. J. Mar. Syst. 17 (1), 179–194.
Fietz, S., Ho, S.L., Huguet, C., 2020. Archaeal membrane lipid-based paleothermometry for applications in polar oceans on JSTOR. Oceanography 33 (2), 104–114.
Fietz, S., Ho, S.L., Huguet, C., Rosell-Melé, A., Martínez-García, A., 2016. Appraising GDGT-based seawater temperature indices in the Southern Ocean. Org. Geochem. 102, 93–105.
Fischer, G., Gersonde, R., Wefer, G., 2002. Organic carbon, biogenic silica and diatom fluxes in the marginal winter sea-ice zone and in the Polar Front Region: interannual variations and differences in composition. Deep Sea Res. Part II 49 (9), 1721–1745.
Fogwill, C.J., Phipps, S.J., Turney, C.S.M., Golledge, N.R., 2015. Sensitivity of the Southern Ocean to enhanced regional Antarctic ice sheet meltwater input. Earth's Future 3 (10), 317–329.
Fok-Pun, L., Komar, P.D., 1983. Settling velocities of planktonic foraminifera; density variations and shape effects. J. Foraminifer. Res. 13 (1), 60–68.
Fraile, I., Schulz, M., Mulitza, S., Kucera, M., 2008. Predicting the global distribution of planktonic foraminifera using a dynamic ecosystem model. Biogeosciences 5 (3), 891–911.
Friedrich, O., Schiebel, R., Wilson, P.A., Weldeab, S., Beer, C.J., Cooper, M.J., Fiebig, J., 2012. Influence of test size, water depth, and ecology on Mg/Ca, Sr/Ca, δ18O and δ13C in nine modern species of planktic foraminifers. Earth Planet Sci. Lett. 319–320, 133–145.
Gemmell, B.J., Oh, G., Buskey, E.J., Villareal, T.A., 2016. Dynamic sinking behaviour in marine phytoplankton: rapid changes in buoyancy may aid in nutrient uptake. Proc. R. Soc. B. 283 (1840), 20161126.
Gilford, D.M., Ashe, E.L., DeConto, R.M., Kopp, R.E., Pollard, D., Rovere, A., 2020. Could the last interglacial constrain projections of future antarctic ice mass loss and sea-level rise? J. Geophys. Res. Earth Surf. 125 (10), e2019JF005418.
Granlí, E., Granéli, W., Rabbani, M.M., Daugbjerg, N., Fransz, G., Roudy, J.C., Alder, V.A., 1993. The influence of copepod and krill grazing on the species composition of phytoplankton communities from the Scotia Weddell sea. Polar Biol. 13 (3), 201–213.
Gray, W.R., Evans, D., 2019. Nonthermal influences on Mg/Ca in planktonic foraminifera: a review of culture studies and application to the last glacial maximum. Paleoceanogr. Paleoclimatol. 34 (3), 306–315.
Greco, M., Jonkers, L., Kretschmer, K., Bijma, J., Kucera, M., 2019. Depth habitat of the planktonic foraminifera Neogloboquadrina pachyderma in the northern high latitudes explained by sea-ice and chlorophyll concentrations. Biogeosciences 16 (17), 3425–3437.
Groeneveld, J., Chiessi, C.M., 2011. Mg/Ca of *Globorotalia inflata* as a recorder of permanent thermocline temperatures in the South Atlantic. Paleoceanography 26 (2), PA2203.
Guiot, J., de Vernal, A., 2011a. Is spatial autocorrelation introducing biases in the apparent accuracy of paleoclimatic reconstructions? Quat. Sci. Rev. 30 (15), 1965–1972.
Guiot, J., de Vernal, A., 2011b. QSR Correspondence "Is spatial autocorrelation introducing biases in the apparent accuracy of palaeoclimatic reconstructions?" Reply to Telford and Birks. Quat. Sci. Rev. 30 (21), 3214–3216.
Haddam, N.A., Michel, E., Siani, G., Cortese, G., Bostock, H.C., Duprat, J.M., Isguder, G., 2016. Improving past sea surface temperature reconstructions from the Southern Hemisphere oceans using planktonic foraminiferal census data. Paleoceanography 31 (6), 822–837.
Harris, R.P., 1994. Zooplankton grazing on the coccolithophore *Emiliania huxleyi* and its role in inorganic carbon flux. Mar. Biol. 119 (3), 431–439.
Hatté, C., Hodgins, G., Jull, A.J.T., Bishop, B., Tesson, B., 2008. Marine chronology based on 14C dating on diatoms proteins. Mar. Chem. 109 (1), 143–151.
Hayward, B.W., Sabaa, A.T., Kolodziej, A., Crundwell, M.P., Steph, S., Scott, G.H., Neil, H.L., Bostock, H.C., Carter, L., Grenfell, H.R., 2012. Planktic foraminifera-based sea-surface temperature record in the Tasman Sea and history of the Subtropical Front around New Zealand, over the last one million years. Mar. Micropaleontol. 82–83, 13–27.
Herbert, T.D., 2003. 6.15 - alkenone paleotemperature determinations. In: Treatise on Geochemistry, ume 6. Pergamon, Oxford, England, UK, pp. 391–432.
Hernández-Almeida, I., Boltovskoy, D., Kruglikova, S.B., Cortese, G., 2020. A new radiolarian transfer function for the Pacific Ocean and application to fossil records: assessing potential and limitations for the last glacial-interglacial cycle. Global Planet. Change 190, 103186.
Hernández-Sánchez, M.T., Woodward, E.M.S., Taylor, K.W.R., Henderson, G.M., Pancost, R.D., 2014. Variations in GDGT distributions through the water column in the south east atlantic ocean. Geochem. Cosmochim. Acta 132, 337–348.
Ho, S.L., Laepple, T., 2016. Flat meridional temperature gradient in the early Eocene in the subsurface rather than surface ocean - nature Geoscience. Nat. Geosci. 9 (8), 606–610.
Ho, S.L., Mollenhauer, G., Fietz, S., Martínez-Garcia, A., Lamy, F., Rueda, G., Schipper, K., Méheust, M., Rosell-Melé, A., Stein, R., Tiedemann, R., 2014. Appraisal of TEX86 and TEX86L thermometries in subpolar and polar regions. Geochem. Cosmochim. Acta 131, 213–226.
Ho, S.L., Mollenhauer, G., Lamy, F., Martínez-Garcia, A., Mohtadi, M., Gersonde, R., Hebbeln, D., Nunez-Ricardo, S., Rosell-Melé, A., Tiedemann, R., 2012. Sea surface temperature variability in the Pacific sector of the Southern Ocean over the past 700 kyr. Paleoceanography 27 (4), PA4202.
Hoffman, J.S., Clark, P.U., Parnell, A.C., He, F., 2017. Regional and global sea-surface temperatures during the last interglaciation. Science 355 (6322), 276–279.
Howard, W.R., Prell, W.L., 1992. Late quaternary surface circulation of the southern Indian ocean and its relationship to orbital variations. Paleoceanography 7 (1), 79–117.
Huguet, C., Fietz, S., Rosell-Melé, A., 2013. Global distribution patterns of hydroxy glycerol dialkyl glycerol tetraethers. Org. Geochem. 57, 107–118.
Hunt, G.L., Drinkwater, K.F., Arrigo, K., Berge, J., Daly, K.L., Danielson, S., Daase, M., Hop, H., Isla, E., Karnovsky, N., Laidre, K., Mueter, F.J., Murphy, E.J., Renaud, P.E., Smith, W.O., Trathan, P., Turner, J., Wolf-Gladrow, D., 2016. Advection in polar and sub-polar environments: impacts on high latitude marine ecosystems. Prog. Oceanogr. 149, 40–81.
Hurley, S.J., Elling, F.J., Könneke, M., Buchwald, C., Wankel, S.D., Santoro, A.E., Lipp, J.S., Hinrichs, K.-U., Pearson, A., 2016. Influence of ammonia oxidation rate on thaumarchaeal lipid composition and the TEX86 temperature proxy. Proc. Natl. Acad. Sci. U.S.A. 113 (28), 7762–7767.
Hutson, W.H., 1980. The agulhas current during the late pleistocene: analysis of modern faunal analogs. Science 207 (4426), 64–66.
Imbrie, J., Kipp, N.J., 1971. A new micropaleontological method for quantitative paleoclimatology: application to a late Pleistocene Caribbean core. In: Turekian, K. (Ed.), The Late Cenozoic Glacial Ages. Yale Univ. Press, Connecticut, USA, pp. 71–181.
Iversen, M.H., Ploug, H., 2010. Ballast minerals and the sinking carbon flux in the ocean: carbon-specific respiration rates and sinking velocity of marine snow aggregates. Biogeosciences 7 (9), 2613–2624.
Jaeschke, A., Wengler, M., Hefter, J., Ronge, T.A., Geibert, W., Mollenhauer, G., Gersonde, R., Lamy, F., 2017. A biomarker perspective on dust, productivity, and sea surface temperature in the Pacific sector of the Southern Ocean. Geochem. Cosmochim. Acta 204, 120–139.
Jiang, L.-Q., Carter, B.R., Feely, R.A., Lauvset, S.K., Olsen, A., 2019. Surface ocean pH and buffer capacity: past, present and future. Sci. Rep. 9 (18624), 1–11.
Jonkers, L., Kučera, M., 2015. Global analysis of seasonality in the shell flux of extant planktonic Foraminifera. Biogeosciences 12 (7), 2207–2226.
Jonkers, L., Kučera, M., 2017. Quantifying the effect of seasonal and vertical habitat tracking on planktonic foraminifera proxies. Clim. Past 13 (6), 573–586.
Jouzel, J., Masson-Delmotte, V., Cattani, O., Dreyfus, G., Falourd, S., Hoffmann, G., Minster, B., Nouet, J., Barnola, J.M., Chappellaz, J., Fischer, H., Gallet, J.C., Johnsen, S., Leuenberger, M., Loulergue, L., Luethi, D., Oerter, H., Parrenin, F., Raisbeck, G., Raynaud, D., Schilt, A., Schwander, J., Selmo, E., Souchez, R., Spahni, R., Stauffer, B., Steffensen, J.P., Stenni, B., Stocker, T.F., Tison, J.L., Werner, M., Wolff, E.W., 2007. Orbital and millennial antarctic climate variability over the past 800,000 years. Science 317 (5839), 793–796.
Karner, M.B., DeLong, E.F., Karl, D.M., 2001. Archaeal dominance in the mesopelagic zone of the Pacific ocean - nature. Nature 409 (6819), 507–510.
Kim, J.-H., Crosta, X., Michel, E., Schouten, S., Duprat, J., Damsté, J.S.S., 2009. Impact of lateral transport on organic proxies in the Southern Ocean. Quat. Res. 71 (2), 246–250.
Kim, J.-H., Crosta, X., Willmott, V., Renssen, H., Bonnin, J., Helmke, P., Schouten, S., Damsté, J.S.S., 2012. Holocene subsurface temperature variability in the eastern Antarctic continental margin. Geophys. Res. Lett. 39 (6).
Kim, J.-H., Schouten, S., Hopmans, E.C., Donner, B., Sinninghe Damsté, J.S., 2008. Global sediment core-top calibration of the TEX86 paleothermometer in the ocean. Geochem. Cosmochim. Acta 72 (4), 1154–1173.
Kim, J.-H., van der Meer, J., Schouten, S., Helmke, P., Willmott, V., Sangiorgi, F., Koç, N., Hopmans, E.C., Damsté, J.S.S., 2010. New indices and calibrations derived from the distribution of crenarchaeal isoprenoid tetraether lipids: implications for past sea surface temperature reconstructions. Geochem.

Cosmochim. Acta 74 (16), 4639–4654.
Kim, Y.S., Orsi, A.H., 2014. On the variability of antarctic circumpolar current fronts inferred from 1992–2011 altimetry. J. Phys. Oceanogr. 44 (12), 3054–3071.
Kimoto, K., 2015. Planktic foraminifera. In: Marine Protists: Diversity and Dynamics. Springer, Tokyo, Japan, pp. 129–178.
King, A.L., Howard, W.R., 2005. δ18O seasonality of planktonic foraminifera from Southern Ocean sediment traps: latitudinal gradients and implications for paleoclimate reconstructions. Mar. Micropaleontol. 56 (1), 1–24.
Kjæret, A.H., Naustvoll, L.-J., Paasche, E., 2000. Ecology of the heterotrophic dinoflagellate genus Protoperidinium in the inner Oslofjord (Norway). Sarsia 85 (5–6), 453–460.
Kopp, R.E., Simons, F.J., Mitrovica, J.X., Maloof, A.C., Oppenheimer, M., 2009. Probabilistic assessment of sea level during the last interglacial stage. Nature 462 (7275), 863–867.
Kučera, M., Weinelt, M., Kiefer, T., Pflaumann, U., Hayes, A., Weinelt, M., Chen, M.-T., Mix, A.C., Barrows, T.T., Cortijo, E., Duprat, J., Juggins, S., Waelbroeck, C., 2005. Reconstruction of sea-surface temperatures from assemblages of planktonic foraminifera: multi-technique approach based on geographically constrained calibration data sets and its application to glacial Atlantic and Pacific Oceans. Quat. Sci. Rev. 24 (7), 951–998.
Kunioka, D., Shirai, K., Takahata, N., Sano, Y., Toyofuku, T., Ujiie, Y., 2006. Microdistribution of Mg/Ca, Sr/Ca, and Ba/Ca ratios in Pulleniatina obliquiloculata test by using a NanoSIMS: implication for the vital effect mechanism. G-cubed 7 (12), Q12P20.
Kusch, S., Eglinton, T.I., Mix, A.C., Mollenhauer, G., 2010. Timescales of lateral sediment transport in the Panama Basin as revealed by radiocarbon ages of alkenones, total organic carbon and foraminifera. Earth Planet Sci. Lett. 290 (3), 340–350.
Lafond, A., Leblanc, K., Legras, J., Cornet, V., Quéguiner, B., 2020. The structure of diatom communities constrains biogeochemical properties in surface waters of the Southern Ocean (Kerguelen Plateau). J. Mar. Syst. 212, 103458.
Laurenceau-Cornec, E.C., Trull, T.W., Davies, D.M., De La Rocha, C.L., Blain, S., 2015. Phytoplankton morphology controls on marine snow sinking velocity. Mar. Ecol. Prog. Ser. 520, 35–56.
Lecourt, M., Muggli, D.L., Harrison, P.J., 1996. Comparison of growth and sinking rates of non-coccolith- and coccolith-forming strains of *Emiliania huxleyi* (Prymnesiophycaea) grown under different irraniances and nitrogen sources. J. Phycol. 32 (1), 17–21.
Lessa, D., Morard, R., Jonkers, L., Venancio, I.M., Reuter, R., Baumeister, A., Albuquerque, A.L., Kucera, M., 2020. Distribution of planktonic foraminifera in the subtropical South Atlantic: depth hierarchy of controlling factors. Biogeosciences 17 (16), 4313–4342.
Lincoln, S.A., Wai, B., Eppley, J.M., Church, M.J., Summons, R.E., DeLong, E.F., 2014. Planktonic Euryarchaeota are a significant source of archaeal tetraether lipids in the ocean. Proc. Natl. Acad. Sci. U.S.A. 111 (27), 9858–9863.
Liu, R., Han, Z., Zhao, J., Zhang, H., Li, D., Ren, J., Pan, J., Zhang, H., 2020. Distribution and source of glycerol dialkyl glycerol tetraethers (GDGTs) and the applicability of GDGT-based temperature proxies in surface sediments of Prydz Bay, East Antarctica. Polar Res. 39.
Liu, X., Lipp, J.S., Hinrichs, K.-U., 2011. Distribution of intact and core GDGTs in marine sediments. Org. Geochem. 42 (4), 368–375.
Locarnini, R.A., Mishonov, A.V., Baranova, O.K., Boyer, T.P., Zweng, M.M., Garcia, H.E., Reagan, J.R., Seidov, D., Weathers, K., Paver, C.R., Smolyar, I., 2018. World ocean atlas 2018, volume 1: Temperature. In: Mishonov, A. (Ed.), NOAA Atlas NESDIS 81. NOAA.
Lüer, V., Cortese, G., Neil, H.L., Hollis, C.J., Willems, H., 2009. Radiolarian-based sea surface temperatures and paleoceanographic changes during the Late Pleistocene–Holocene in the subantarctic southwest Pacific. Mar. Micropaleontol. 70 (3), 151–165.
Mackie, S., Smith, I.J., Ridley, J.K., Stevens, D.P., Langhorne, P.J., 2020. Climate response to increasing antarctic iceberg and ice shelf melt. J. Clim. 33 (20), 8917–8938.
Malevich, S.B., Vetter, L., Tierney, J.E., 2019. Global core top calibration of δ18O in planktic foraminifera to sea surface temperature. Paleoceanogr. Paleoclimatol. 34 (8), 1292–1315.
Marr, J.P., Baker, J.A., Carter, L., Allan, A.S.R., Dunbar, G.B., Bostock, H.C., 2011. Ecological and temperature controls on Mg/Ca ratios of Globigerina bulloides from the southwest Pacific Ocean. Paleoceanography 26 (2).
Marret, F., de Vernal, A., Benderra, F., Harland, R., 2001. Late Quaternary sea-surface conditions at DSDP Hole 594 in the southwest Pacific Ocean based on dinoflagellate cyst assemblages. J. Quat. Sci. 16 (7), 739–751.
Martin, J.H., 1990. Glacial-interglacial CO2 change: the iron Hypothesis. Paleoceanography 5 (1), 1–13.
Martínez-Garcia, A., Rosell-Melé, A., Geibert, W., Gersonde, R., Masqué, P., Gaspari, V., Barbante, C., 2009. Links between iron supply, marine productivity, sea surface temperature, and CO2 over the last 1.1 Ma. Paleoceanography 24 (1).
Mashiotta, T.A., Lea, D.W., Spero, H.J., 1999. Glacial–interglacial changes in Subantarctic sea surface temperature and δ18O-water using foraminiferal Mg. Earth Planet Sci. Lett. 170 (4), 417–432.
Masson-Delmotte, V., Buiron, D., Ekaykin, A., Frezzotti, M., Gallée, H., Jouzel, J., Krinner, G., Landais, A., Motoyama, H., Oerter, H., Pol, K., Pollard, D., Ritz, C., Schlosser, E., Sime, L.C., Sodemann, H., Stenni, B., Uemura, R., Vimeux, F., 2011. A comparison of the present and last interglacial periods in six Antarctic ice cores. Clim. Past 7 (2), 397–423.
McDonnell, A.M.P., Buesseler, K.O., 2010. Variability in the average sinking velocity of marine particles. Limnol. Oceanogr. 55 (5), 2085–2096.
Meilland, J., Fabri-Ruiz, S., Koubbi, P., Monaco, C.L., Cotte, C., Hosie, G.W., Sanchez, S., Howa, H., 2016. Planktonic foraminiferal biogeography in the Indian sector of the Southern Ocean: contribution from CPR data. Deep Sea Res. Part I 110, 75–89.
Mekik, F., 2014. Radiocarbon dating of planktonic foraminifer shells: a cautionary tale. Paleoceanography 29 (1), 13–29.
Mercer, J.H., 1978. West Antarctic ice sheet and CO2 greenhouse effect: a threat of disaster. Nature 271 (5643), 321–325.
Miklasz, K.A., Denny, M.W., 2010. Diatom sinkings speeds: improved predictions and insight from a modified Stokes' law. Limnol. Oceanogr. 55 (6), 2513–2525.
Mollenhauer, G., Eglinton, T.I., Hopmans, E.C., Sinninghe Damsté, J.S., 2008. A radiocarbon-based assessment of the preservation characteristics of crenarchaeol and alkenones from continental margin sediments. Org. Geochem. 39 (8), 1039–1045.
Mollenhauer, G., Kienast, M., Lamy, F., Meggers, H., Schneider, R.R., Hayes, J.M., Eglinton, T.I., 2005. An evaluation of 14C age relationships between co-occurring foraminifera, alkenones, and total organic carbon in continental margin sediments. Paleoceanography 20 (1).
Mortyn, P.G., Charles, C.D., 2003. Planktonic foraminiferal depth habitat and δ18O calibrations: plankton tow results from the Atlantic sector of the Southern Ocean. Paleoceanography 18 (2).
Müller, P.J., Kirst, G., Ruhland, G., von Storch, I., Rosell-Melé, A., 1998. Calibration of the alkenone paleotemperature index U37K′ based on core-tops from the eastern South Atlantic and the global ocean (60°N-60°S). Geochem. Cosmochim. Acta 62 (10), 1757–1772.
Nardelli, B.B., Guinehut, S., Verbrugge, N., Cotroneo, Y., Zambianchi, E., Iudicone, D., 2017. Southern Ocean mixed-layer seasonal and interannual variations from combined satellite and in situ data. J. Geophys. Res. Oceans 122 (12), 10042–10060.
Niebler, H.-S., Gersonde, R., 1998. A planktic foraminiferal transfer function for the southern South Atlantic Ocean. Mar. Micropaleontol. 34 (3), 213–234.
Nishimura, A., Nakaseko, K., 2011. Characterization of radiolarian assemblages in the surface sediments of the Antarctic Ocean. Palaeoworld 20 (2), 232–251.
Nissen, C., Vogt, M., Münnich, M., Gruber, N., Haumann, F.A., 2018. Factors controlling coccolithophore biogeography in the Southern Ocean. Biogeosciences 15 (22), 6997–7024.
Nooteboom, P.D., Bijl, P.K., van Sebille, E., von der Heydt, A.S., Dijkstra, H.A., 2019. Transport bias by ocean currents in sedimentary microplankton assemblages: implications for paleoceanographic reconstructions. Paleoceanogr. Paleoclimatol. 34 (7), 1178–1194.
Nunes, S., Latasa, M., Delgado, M., Emelianov, M., Simó, R., Estrada, M., 2019. Phytoplankton community structure in contrasting ecosystems of the Southern Ocean: south Georgia, south orkneys and western antarctic peninsula. Deep Sea Res. Part I 151, 103059.
Ohkouchi, N., Eglinton, T.I., Keigwin, L.D., Hayes, J.M., 2002. Spatial and temporal offsets between proxy records in a sediment drift. Science 298 (5596).
Ortiz, J.D., Mix, A.C., 1997. Comparison of Imbrie-Kipp Transfer Function and modern analog temperature estimates using sediment trap and core top foraminiferal faunas. Paleoceanography 12 (2), 175–190.
Overpeck, J.T., Webb, T., Prentice, I.C., 1985. Quantitative interpretation of fossil pollen spectra: dissimilarity coefficients and the method of modern analogs. Quat. Res. 23 (1), 87–108.
Pahnke, K., Sachs, J.P., 2006. Sea surface temperatures of southern midlatitudes 0–160 kyr B.P. Paleoceanography 21 (2).
Pan, H., Sun, M.-Y., 2011. Variations of alkenone based paleotemperature index (U37K′) during Emiliania huxleyi cell growth, respiration (auto-metabolism) and microbial degradation. Org. Geochem. 42 (6), 678–687.
Panassa, E., Völker, C., Wolf-Gladrow, D., Hauck, J., 2018. Drivers of interannual variability of summer mixed layer depth in the Southern Ocean between 2002 and 2011. J. Geophys. Res. Oceans 123 (8), 5077–5090.
Park, E., Hefter, J., Fischer, G., Iversen, M.H., Ramondenc, S., Nöthig, E.-M., Mollenhauer, G., 2019a. Seasonality of archaeal lipid flux and GDGT-based thermometry in sinking particles of high-latitude oceans: fram Strait (79° N) and Antarctic Polar Front (50°S). Biogeosciences 16 (11), 2247–2268.
Park, Y.-H., Park, T., Kim, T.-W., Lee, S.-H., Hong, C.-S., Lee, J.-H., Rio, M.-H., Pujol, M.-I., Ballarotta, M., Durand, I., Provost, C., 2019b. Observations of the antarctic circumpolar current over the udintsev fracture zone, the narrowest choke point in the Southern Ocean. J. Geophys. Res. Oceans 124 (7), 4511–4528.
Passow, U., 1991. Species-specific sedimentation and sinking velocities of diatoms. Mar. Biol. 108 (3), 449–455.
Passow, U., French, M.A., Robert, M., 2011. Biological controls on dissolution of diatom frustules during their descent to the deep ocean: lessons learned from controlled laboratory experiments. Deep Sea Res. Part I 58 (12), 1147–1157.
Pelejero, C., Calvo, E., Barrows, T.T., Logan, G.A., De Deckker, P., 2006. South Tasman Sea alkenone palaeothermometry over the last four glacial/interglacial cycles. Mar. Geol. 230 (1), 73–86.
Petit, J.R., Jouzel, J., Raynaud, D., Barkov, N.I., Barnola, J.-M., Basile, I., Bender, M., Chappellaz, J., Davis, M., Delaygue, G., Delmotte, M., Kotlyakov, V.M., Legrand, M., Lipenkov, V.Y., Lorius, C., PÉpin, L., Ritz, C., Saltzman, E., Stievenard, M., 1999. Climate and atmospheric history of the past 420,000 years from the Vostok ice core, Antarctica. Nature 399 (6735), 429–436.
Ploug, H., Iversen, M.H., Fischer, G., 2008. Ballast, sinking velocity, and apparent diffusivity within marine snow and zooplankton fecal pellets: implications for substrate turnover by attached bacteria. Limnol. Oceanogr. 53 (5), 1878–1886.

Popova, I.M., 1986. Transportation of radiolarian shells by currents (calculations based on the example of the Kuroshio). Mar. Micropaleontol. 11 (1), 197–201.
Prahl, F.G., Mix, A.C., Sparrow, M.A., 2006. Alkenone paleothermometry: biological lessons from marine sediment records off western South America. Geochem. Cosmochim. Acta 70 (1), 101–117.
Prahl, F.G., Muehlhausen, L.A., Zahnle, D.L., 1988. Further evaluation of long-chain alkenones as indicators of paleoceanographic conditions. Geochem. Cosmochim. Acta 52 (9), 2303–2310.
Prahl, F.G., Rontani, J.-F., Zabeti, N., Walinsky, S.E., Sparrow, M.A., 2010. Systematic pattern in U37K′ – temperature residuals for surface sediments from high latitude and other oceanographic settings. Geochem. Cosmochim. Acta 74 (1), 131–143.
Prahl, F.G., Wakeham, S.G., 1987. Calibration of unsaturation patterns in long-chain ketone compositions for palaeotemperature assessment. Nature 330 (6146), 367–369.
Prebble, J.G., Crouch, E.M., Carter, L., Cortese, G., Bostock, H., Neil, H., 2013a. An expanded modern dinoflagellate cyst dataset for the Southwest Pacific and Southern Hemisphere with environmental associations. Mar. Micropaleontol. 101, 33–48.
Prebble, J.G., Crouch, E.M., Carter, L., Cortese, G., Nodder, S.D., 2013b. Dinoflagellate cysts from two sediment traps east of New Zealand. Mar. Micropaleontol. 104, 25–37.
Qin, W., Carlson, L.T., Armbrust, E.V., Devol, A.H., Moffett, J.W., Stahl, D.A., Ingalls, A.E., 2015. Confounding effects of oxygen and temperature on the TEX86 signature of marine Thaumarchaeota. Proc. Natl. Acad. Sci. U.S.A. 112 (35), 10979–10984.
Quéguiner, B., 2013. Iron fertilization and the structure of planktonic communities in high nutrient regions of the Southern Ocean. Deep Sea Res. Part II 90, 43–54.
Raffi, I., Backman, J., Fornaciari, E., Pälike, H., Rio, D., Lourens, L., Hilgen, F., 2006. A review of calcareous nannofossil astrobiochronology encompassing the past 25 million years. Quat. Sci. Rev. 25 (23), 3113–3137.
Rahul, M., Shetye Suhas, S., Manish, T., Narayanpillai, A., 2015. Secondary calcification of planktic foraminifera from the Indian sector of Southern Ocean. Acta Geologica Sinica -. English Edition 89 (1), 27–37.
Rama-Corredor, O., Cortina, A., Martrat, B., Lopez, J.F., Grimalt, J.O., 2018. Removal of bias in C37 alkenone-based sea surface temperature measurements by high-performance liquid chromatography fractionation. J. Chromatogr. A 1567, 90–98.
Raven, J.A., Waite, A.M., 2004. The evolution of silicification in diatoms: inescapable sinking and sinking as escape? New Phytol. 162 (1), 45–61.
Regenberg, M., Regenberg, A., Garbe-Schönberg, D., Lea, D.W., 2014. Global dissolution effects on planktonic foraminiferal Mg/Ca ratios controlled by the calcite-saturation state of bottom waters. Paleoceanography 29 (3), 127–142.
Rembauville, M., Blain, S., Armand, L., Quéguiner, B., Salter, I., 2015. Export fluxes in a naturally iron-fertilized area of the Southern Ocean – Part 2: importance of diatom resting spores and faecal pellets for export. Biogeosciences 12 (11), 3171–3195.
Renaud, S., Schmidt, D.N., 2003. Habitat tracking as a response of the planktic foraminifer Globorotalia truncatulinoides to environmental fluctuations during the last 140 kyr. Mar. Micropaleontol. 49 (1), 97–122.
Rigual-Hernández, A.S., Trull, T.W., Bray, S.G., Armand, L.K., 2016. The fate of diatom valves in the Subantarctic and Polar Frontal Zones of the Southern Ocean: sediment trap versus surface sediment assemblages. Palaeogeogr. Palaeoclimatol. Palaeoecol. 457, 129–143.
Rintoul, S.R., 2018. The global influence of localized dynamics in the Southern Ocean. Nature 558 (7709), 209–218.
Roberts, J., McCave, I.N., McClymont, E.L., Kender, S., Hillenbrand, C.-D., Matano, R., Hodell, D.A., Peck, V.L., 2017. Deglacial changes in flow and frontal structure through the Drake Passage. Earth Planet Sci. Lett. 474, 397–408.
Rodrigo-Gámiz, M., Rampen, S.W., de Haas, H., Baas, M., Schouten, S., Sinninghe Damsté, J.S., 2015. Constraints on the applicability of the organic temperature proxies UK'37, TEX86 and LDI in the subpolar region around Iceland. Biogeosciences 12 (22), 6573–6590.
Romero, O.E., Armand, L.K., Crosta, X., Pichon, J.-J., 2005. The biogeography of major diatom taxa in Southern Ocean surface sediments: 3. Tropical/Subtropical species. Palaeogeogr. Palaeoclimatol. Palaeoecol. 223 (1), 49–65.
Rongstad, B.L., Marchitto, T.M., Herguera, J.C., 2017. Understanding the effects of dissolution on the Mg/Ca paleothermometer in planktic foraminifera: evidence from a novel individual foraminifera method. Paleoceanography 32 (12), 1386–1402.
Rontani, J.-F., Volkman, J.K., Prahl, F.G., Wakeham, S.G., 2013. Biotic and abiotic degradation of alkenones and implications for U37K′ paleoproxy applications: a review. Org. Geochem. 59, 95–113.
Rosas-Navarro, A., Langer, G., Ziveri, P., 2018. Temperature effects on sinking velocity of different *Emiliania huxleyi* strains. PloS One 13 (3), e0194386.
Rosell-Melé, A., Prahl, F.G., 2013. Seasonality of UK'37 temperature estimates as inferred from sediment trap data. Quat. Sci. Rev. 72, 128–136.
Rosenthal, Y., Perron-Cashman, S., Lear, C.H., Bard, E., Barker, S., Billups, K., Bryan, M., Delaney, M.L., DeMenocal, P.B., Dwyer, G.S., Elderfield, H., German, C.R., Greaves, M., Lea, D.W., Marchitto, T.M., Pak, D.K., Paradis, G.L., Russell, A.D., Schneider, R.R., Scheiderich, K., Stott, L., Tachikawa, K., Tappa, E., Thunell, R., Wara, M., Weldeab, S., Wilson, P.A., 2004. Interlaboratory comparison study of Mg/Ca and Sr/Ca measurements in planktonic foraminifera for paleoceanographic research. G-cubed 5 (4).
Rühlemann, C., Butzin, M., 2006. Alkenone temperature anomalies in the Brazil-Malvinas Confluence area caused by lateral advection of suspended particulate material. G-cubed 7 (10).
Sachs, J.P., Anderson, R.F., 2003. Fidelity of alkenone paleotemperatures in southern Cape Basin sediment drifts. Paleoceanography 18 (4).
Sadekov, A. Yu, Eggins, S.M., De Deckker, P., 2005. Characterization of Mg/Ca distributions in planktonic foraminifera species by electron microprobe mapping. G-cubed 6 (12).
Saenger, C.P., Evans, M.N., 2019. Calibration and validation of environmental controls on planktic foraminifera Mg/Ca using global core-top data. Paleoceanogr. Paleoclimatol. 34 (8), 1249–1270.
Salvinac, 1998. Variabilité hydrologiques et climatique de l'Océan Austral (secteur indien) au cours du Quaternaire terminal. Essai de corrélations inter-hémisphériques. Ph. D. thesis. Univ. de Bordeaux.
Samtleben, C., 1980. Die Evolution der Coccolithophoriden-GattungGephyrocapsa nach Befunden im Atlantik. Paläontol. Z. 54 (1), 91–127.
Schaefer, G., Rodger, J.S., Hayward, B.W., Kennett, J.P., Sabaa, A.T., Scott, G.H., 2005. Planktic foraminiferal and sea surface temperature record during the last 1 Myr across the Subtropical Front, Southwest Pacific. Mar. Micropaleontol. 54 (3), 191–212.
Scherer, R.P., Aldahan, A., Tulaczyk, S., Possnert, G., Engelhardt, H., Kamb, B., 1998. Pleistocene collapse of the West Antarctic ice sheet. Science 281 (5373), 82–85.
Schlüter, L., Henriksen, P., Nielsen, T.G., Jakobsen, H.H., 2011. Phytoplankton composition and biomass across the southern Indian Ocean. Deep Sea Res. Part I 58 (5), 546–556.
Schmidt, K., De La Rocha, C.L., Gallinari, M., Cortese, G., 2014. Not all calcite ballast is created equal: differing effects of foraminiferan and coccolith calcite on the formation and sinking of aggregates. Biogeosciences 11 (1), 135–145.
Schouten, S., Hopmans, E.C., Schefuß, E., Sinninghe Damsté, J.S., 2002. Distributional variations in marine crenarchaeotal membrane lipids: a new tool for reconstructing ancient sea water temperatures? Earth Planet Sci. Lett. 204 (1), 265–274.
Schouten, S., Hopmans, E.C., Sinninghe Damsté, J.S., 2013. The organic geochemistry of glycerol dialkyl glycerol tetraether lipids: a review. Org. Geochem. 54, 19–61.
Shackleton, N.J., 1974. Attainment of Isotopic Equilibrium between Ocean Water and the Benthonic Foraminifera Genus Uvigerina: Isotopic Changes in the Ocean during the Last Glacial, ume 219. C.N.R.S. Colloquium, pp. 203–209.
Shah, S.R., Mollenhauer, G., Ohkouchi, N., Eglinton, T.I., Pearson, A., 2008. Origins of archaeal tetraether lipids in sediments: insights from radiocarbon analysis. Geochem. Cosmochim. Acta 72 (18), 4577–4594.
Shanks, A.L., Trent, J.D., 1980. Marine snow: sinking rates and potential role in vertical flux. Deep Sea Res. Part A 27 (2), 137–143.
Shevenell, A.E., Ingalls, A.E., Domack, E.W., Kelly, C., 2011. Holocene Southern Ocean surface temperature variability west of the antarctic peninsula - nature. Nature 470 (7333), 250–254.
Sicre, M.A., Labeyrie, L., Ezat, U., Duprat, J., Turon, J.L., Schmidt, S., Michel, E., Mazaud, A., 2005. Mid-latitude southern Indian ocean response to northern Hemisphere heinrich events. Earth Planet Sci. Lett. 240 (3), 724–731.
Sikes, E.L., Howard, W.R., Samson, C.R., Mahan, T.S., Robertson, L.G., Volkman, J.K., 2009. Southern Ocean seasonal temperature and subtropical front movement on the south tasman rise in the late quaternary. Paleoceanography 24 (2).
Sikes, E.L., O'Leary, T., Nodder, S.D., Volkman, J.K., 2005. Alkenone temperature records and biomarker flux at the subtropical front on the chatham rise, SW Pacific Ocean. Deep Sea Res. Part I 52 (5), 721–748.
Sikes, E.L., Volkman, J.K., 1993. Calibration of alkenone unsaturation ratios (UK'37) for paleotemperature estimation in cold polar waters. Geochem. Cosmochim. Acta 57 (8), 1883–1889.
Sikes, E.L., Volkman, J.K., Robertson, L.G., Pichon, J.-J., 1997. Alkenones and alkenes in surface waters and sediments of the Southern Ocean: implications for paleotemperature estimation in polar regions. Geochem. Cosmochim. Acta 61 (7), 1495–1505.
Small, L.F., Fowler, S.W., Ünlü, M.Y., 1979. Sinking rates of natural copepod fecal pellets. Mar. Biol. 51 (3), 233–241.
Smetacek, V., Assmy, P., Henjes, J., 2004. The role of grazing in structuring Southern Ocean pelagic ecosystems and biogeochemical cycles. Antarct. Sci. 16 (4), 541–558.
Smetacek, V.S., 1985. Role of sinking in diatom life-history cycles: ecological, evolutionary and geological significance. Mar. Biol. 84 (3), 239–251.
Spencer-Jones, C.L., McClymont, E.L., Bale, N.J., Hopmans, E.C., Schouten, S., Müller, J., Abrahamsen, E.P., Allen, C., Bickert, T., Hillenbrand, C.-D., Mawbey, E., Peck, V., Svalova, A., Smith, J.A., 2021. Archaeal intact polar lipids in polar waters: a comparison between the Amundsen and Scotia seas. Biogeosciences 18 (11), 3485–3504.
Stoecker, D.K., Johnson, M.D., de Vargas, C., Not, F., 2009. Acquired phototrophy in aquatic protists. Aquat. Microb. Ecol. 57 (3), 279–310.
Sun, B., Liu, C., Wang, F., 2019. Global meridional eddy heat transport inferred from Argo and altimetry observations. Sci. Rep. 9 (1345), 1–10.
Sutter, J., Gierz, P., Grosfeld, K., Thoma, M., Lohmann, G., 2016. ocean temperature thresholds for last interglacial West Antarctic ice sheet collapse. Geophys. Res. Lett. 43 (6), 2675–2682.
Takahashi, K., Be, A.W.H., 1984. Planktonic foraminifera: factors controlling sinking speeds. Deep Sea Res. Part A 31 (12), 1477–1500.
Takahashi, K., Honjo, S., 1983. Radiolarian skeletons: size, weight, sinking speed, and residence time in tropical pelagic oceans. Deep Sea Res. Part A 30 (5), 543–568.
Taylor, K.W.R., Huber, M., Hollis, C.J., Hernandez-Sanchez, M.T., Pancost, R.D., 2013.

Re-evaluating modern and Palaeogene GDGT distributions: implications for SST reconstructions. Global Planet. Change 108, 158–174.
Telford, R.J., Birks, H.J.B., 2011. QSR Correspondence "Is spatial autocorrelation introducing biases in the apparent accuracy of palaeoclimatic reconstructions?". Quat. Sci. Rev. 30 (21), 3210–3213.
Thierstein, H.R., Geitzenauer, K.R., Molfino, B., Shackleton, N.J., 1977. Global synchroneity of late Quaternary coccolith datum levels Validation by oxygen isotopes. Geology 5 (7), 400–404.
Tierney, J.E., Malevich, S.B., Gray, W., Vetter, L., Thirumalai, K., 2019. Bayesian calibration of the Mg/Ca paleothermometer in planktic foraminifera. Paleoceanogr. Paleoclimatol. 34 (12), 2005–2030.
Tierney, J.E., Tingley, M.P., 2014. A Bayesian, spatially-varying calibration model for the TEX86 proxy. Geochem. Cosmochim. Acta 127, 83–106.
Tierney, J.E., Tingley, M.P., 2015. A TEX86 surface sediment database and extended Bayesian calibration. Sci. Data 2 (150029), 1–10.
Tierney, J.E., Tingley, M.P., 2018. BAYSPLINE: a new calibration for the alkenone paleothermometer. Paleoceanogr. Paleoclimatol. 33 (3), 281–301.
Turney, C.S.M., Fogwill, C.J., Golledge, N.R., McKay, N.P., van Sebille, E., Jones, R.T., Etheridge, D., Rubino, M., Thornton, D.P., Davies, S.M., Ramsey, C.B., Thomas, Z.A., Bird, M.I., Munksgaard, N.C., Kohno, M., Woodward, J., Winter, K., Weyrich, L.S., Rootes, C.M., Millman, H., Albert, P.G., Rivera, A., van Ommen, T., Curran, M., Moy, A., Rahmstorf, S., Kawamura, K., Hillenbrand, C.-D., Weber, M.E., Manning, C.J., Young, J., Cooper, A., 2020a. Early Last Interglacial ocean warming drove substantial ice mass loss from Antarctica. Proc. Natl. Acad. Sci. U.S.A. 117 (8), 3996–4006.
Turney, C.S.M., Jones, R.T., McKay, N.P., van Sebille, E., Thomas, Z.A., Hillenbrand, C.-D., Fogwill, C.J., 2020b. A global mean sea surface temperature dataset for the Last Interglacial (129–116ka) and contribution of thermal expansion to sea level change. Earth Syst. Sci. Data 12 (4), 3341–3356.
Urey, H.C., Lowenstam, H.A., Epstein, S., Mckinney, C.R., 1951. Measurement of paleotemperatures and temperatures of the upper Cretaceous of England, Denmark, and the southeastern United States. GSA Bulletin 62 (4), 399–416.
Vázquez Riveiros, N., Govin, A., Waelbroeck, C., Mackensen, A., Michel, E., Moreira, S., Bouinot, T., Caillon, N., Orgun, A., Brandon, M., 2016. Mg/Ca thermometry in planktic foraminifera: improving paleotemperature estimations for G. bulloides and N. pachyderma left. G-cubed 17 (4), 1249–1264.
van Sebille, E., Scussolini, P., Durgadoo, J.V., Peeters, F.J.C., Biastoch, A., Weijer, W., Turney, C., Paris, C.B., Zahn, R., 2015. Ocean currents generate large footprints in marine palaeoclimate proxies. Nat. Commun. 6 (6521), 1–8.
Vaughan, D.G., 2008. West Antarctic Ice Sheet collapse – the fall and rise of a paradigm. Climatic Change 91 (1), 65–79.
Verleye, T.J., Louwye, S., 2010. Recent geographical distribution of organic-walled dinoflagellate cysts in the southeast Pacific (25–53°S) and their relation to the prevailing hydrographical conditions. Palaeogeogr. Palaeoclimatol. Palaeoecol. 298 (3), 319–340.
Versteegh, G.J.M., Zonneveld, K.A.F., 2002. Use of selective degradation to separate preservation from productivity. Geology 30 (7), 615–618.
Volkov, D.L., Fu, L.-L., Lee, T., 2010. Mechanisms of the meridional heat transport in the Southern Ocean. Ocean Dynam. 60 (4), 791–801.
von Gyldenfeldt, A.-B., Carstens, J., Meincke, J., 2000. Estimation of the catchment area of a sediment trap by means of current meters and foraminiferal tests. Deep Sea Res. Part II 47 (9), 1701–1717.
von Langen, P.J., Pak, D.K., Spero, H.J., Lea, D.W., 2005. Effects of temperature on Mg/Ca in neogloboquadrinid shells determined by live culturing. G-cubed 6 (10).
Walker, M., Hammel, J.U., Wilde, F., Hoehfurtner, T., Humphries, S., Schuech, R., 2021. Estimation of sinking velocity using free-falling dynamically scaled models: foraminifera as a test case. J. Exp. Biol. 224 (2).
Watanabe, O., Jouzel, J., Johnsen, S., Parrenin, F., Shoji, H., Yoshida, N., 2003. Homogeneous climate variability across East Antarctica over the past three glacial cycles. Nature 422 (6931), 509–512.
Weijers, J.W.H., Schouten, S., Spaargaren, O.C., Sinninghe Damsté, J.S., 2006. Occurrence and distribution of tetraether membrane lipids in soils: implications for the use of the TEX86 proxy and the BIT index. Org. Geochem. 37 (12), 1680–1693.
Wheatcroft, R.A., 1992. Experimental tests for particle size-dependent bioturbation in the deep ocean. Limnol. Oceanogr. 37 (1), 90–104.
Wright, S.W., van den Enden, R.L., Pearce, I., Davidson, A.T., Scott, F.J., Westwood, K.J., 2010. Phytoplankton community structure and stocks in the Southern Ocean (30–80°E) determined by CHEMTAX analysis of HPLC pigment signatures. Deep Sea Res. Part II 57 (9), 758–778.
Wuchter, C., Schouten, S., Wakeham, S.G., Damsté, J.S.S., 2005. Temporal and spatial variation in tetraether membrane lipids of marine Crenarchaeota in particulate organic matter: implications for TEX86 paleothermometry. Paleoceanography 20 (3).
Xiao, W., Frederichs, T., Gersonde, R., Kuhn, G., Esper, O., Zhang, X., 2016. Constraining the dating of late quaternary marine sediment records from the scotia sea (Southern Ocean). Quat. Geochronol. 31, 97–118.
Yamamoto, M., Shimamoto, A., Fukuhara, T., Tanaka, Y., Ishizaka, J., 2012. Glycerol dialkyl glycerol tetraethers and TEX86 index in sinking particles in the western North Pacific. Org. Geochem. 53, 52–62.
Yin, Q., Berger, A., 2015. Interglacial analogues of the Holocene and its natural near future. Quat. Sci. Rev. 120, 28–46.
Zhang, Y.G., Pagani, M., Wang, Z., 2016. Ring Index: a new strategy to evaluate the integrity of TEX86 paleothermometry. Paleoceanography 31 (2), 220–232.
Zhang, Y.G., Zhang, C.L., Liu, X.-L., Li, L., Hinrichs, K.-U., Noakes, J.E., 2011. Methane Index: a tetraether archaeal lipid biomarker indicator for detecting the instability of marine gas hydrates. Earth Planet Sci. Lett. 307 (3), 525–534.
Zielinski, U., Gersonde, R., Sieger, R., Fütterer, D., 1998. Quaternary surface water temperature estimations: calibration of a diatom transfer function for the Southern Ocean. Paleoceanography 13 (4), 365–383.
Zonneveld, K.A.F., Bockelmann, F., Holzwarth, U., 2007. Selective preservation of organic-walled dinoflagellate cysts as a tool to quantify past net primary production and bottom water oxygen concentrations. Mar. Geol. 237 (3), 109–126.
Zonneveld, K.A.F., Marret, F., Versteegh, G.J.M., Bogus, K., Bonnet, S., Bouimetarhan, I., Crouch, E., de Vernal, A., Elshanawany, R., Edwards, L., Esper, O., Forke, S., Grøsfjeld, K., Henry, M., Holzwarth, U., Kielt, J.-F., Kim, S.-Y., Ladouceur, S., Ledu, D., Chen, L., Limoges, A., Londeix, L., Lu, S.-H., Mahmoud, M.S., Marino, G., Matsouka, K., Matthiessen, J., Mildenhal, D.C., Mudie, P., Neil, H.L., Pospelova, V., Qi, Y., Radi, T., Richerol, T., Rochon, A., Sangiorgi, F., Solignac, S., Turon, J.-L., Verleye, T., Wang, Y., Wang, Z., Young, M., 2013. Atlas of modern dinoflagellate cyst distribution based on 2405 data points. Rev. Palaeobot. Palynol. 191, 1–197.